Numerical Weather Prediction

An Analysis of CHAMP Radio Occultation Data

Forecasting Research Technical Report No. 471

Axel von Engeln

email:nwp_publications@metoffice.gov.uk

Contents

1 Abstract **5**

2 Introduction **6**

3 CHAMP Data used **7**

4 ECMWF Background used **11**

5 FSI Amplitude Analysis **15**

6 FSI Amplitude Variability Analysis **16**

7 FSI Amplitude Cutoff Analysis **18**

8 Fly Wheeling Analysis **19**

9 Ground Station Analysis **23**

10 GPS Satellite Analysis **26**

11 Processing Centre Analysis **29**

12 Conclusion **33**

13 Acknowledgments **37**

1 Abstract

Radio occultation data provides accurate information on the atmospheric temperature profile at altitudes below about 35 km. Also, information on the water vapour profile at altitudes below about 5 km can be derived from this data. This data will soon be available operationally and thus data monitoring is required. Within this report, CHAMP radio occultation data is analyzed with respect to its FSI amplitude, the ground station involved in double differencing, the GPS occultation satellite and the processing centre providing CHAMP data. The FSI amplitude has characteristics similar to a signal-to-noise ratio and atmospheric features such as the Intertropical Convergence Zone show up. It is also a good measure to filter out occultations that show biases at low altitudes. Data quality with respect to the ground station used in the differencing is mostly in agreement, although some ground stations show distinctly different statistics. Whether this is caused by the actual coverage of a ground station is not yet clear. A similar result holds for the occulting GPS satellite. A comparison of two processing centres providing CHAMP data shows that global results are generally in agreement, with lower standard deviations found at high altitudes. A separation into latitude bands shows significant differences which need to be addressed to reach the full potential of radio occultation for climate monitoring.

Change History

Date	Comment
03/10/2005	First outline presented to D. Offiler (Met Office, UK)
11/11/2005	First draft, partly based on Visiting Scientist proposal for DMI
07/12/2005	Comments by G. Beyerle and J. Wickert (GFZ, Germany) implemented
02/01/2006	Latitude inconsistencies (geodetic or geocentric) resolved with GFZ and CDAAC
06/01/2006	Comments by S. Sokolovskiy (UCAR, USA) implemented
13/01/2006	Fly-wheeling calculation by C. Marquardt (EUMETSAT, Germany) outlined
23/01/2006	NWP Technical Report Number 471 assigned
02/02/2006	Comments by D. Offiler and J. Eyre (Met Office, UK) implemented
03/02/2006	Issued as NWP Technical Report 471

2 Introduction

Radio occultation instruments using Global Positioning System (GPS) signals allow the measurement of the variable vertical refractive index of the atmosphere [9, 16]. A radio occultation instrument is usually located on a LEO (low earth orbiting) satellite and observes the GPS satellites in a limb-sounding occultation geometry. The varying density (and thus refractivity) profile of the earth's atmosphere will cause a GPS satellite signal to be refracted (bent) from a straight line. The magnitude of this deviation (called bending angle) depends on the refractivity gradient in the atmosphere, which in turn depends on the temperature and water vapour profile. Further processing of these measurements allows the derivation of temperature, pressure and water vapour profiles, as well as surface pressure. Several radio occultation instruments have already shown the potential of this measurement technique; for an overview on past and future missions, the reader is referred to [28].

The latest processing method for radio occultation data uses the Full Spectrum Inversion (FSI) technique [7] to derive the bending angle profile from the raw measurements. FSI processing is especially important in the lower troposphere where it resolves multi-path. The amplitude of the FSI processing is also often used to assess the quality of the retrieved refractivity profile where processing is stopped when the amplitude drops below a certain threshold.

Radio occultation data will soon be operationally available with the GRAS instrument on MetOp and the COSMIC constellation [4, 17]. Before operational assimilation of this new data type into Numerical Weather Prediction models can start, the data requires close monitoring to assure that the potentially assimilated data fulfills certain quality requirements. Several quality monitoring options are already discussed in [10]. Here, a summary of additional work performed at the Met Office to analyze the quality of radio occultation data is presented. The analysis is based primarily on CHAMP data processed at the GeoForschungsZentrum Potsdam, Germany. The report covers the following topics:

Section 3 Introduces the CHAMP data streams used, along with a general analysis on coverage, signal-to-noise ratio, and horizontal displacement of the tangent point.

Section 4 Introduces the ECMWF dataset used for CHAMP validation purposes, along with an investigation on the impact of the horizontal displacement and the available ECMWF analysis times on the quality of the validation profile.

Section 5 Presents a general analysis of the impact of atmospheric variability on the FSI amplitude.

Section 7 Presents an analysis of the impact of different FSI amplitude cut-off values on the quality of the retrieved refractivity profiles.

Section 6 Presents an analysis on the vertical variability of the FSI amplitude.

Section 8 Presents an analysis on the amount of fly-wheeling found in the CHAMP radio occultation data. Fly-wheeling is an indicator of GPS tracking loss-of-lock.

Section 9 Presents an analysis of the retrieved refractivity profile depending on the ground station used for double differencing.

Section 10 Presents an analysis of the retrieved refractivity profile depending on the occulting GPS satellite.

Section 11 Presents an analysis of the difference in the retrieved refractivity profile between two processing centres.

Section 12 Presents the conclusion.

3 CHAMP Data used

Four different sets of CHAMP data streams are used in this analysis. Two are operational streams from the processing centres GFZ (GeoForschungsZentrum Potsdam, Germany) and from CDAAC (COSMIC Data Analysis and Archive Center, Boulder, USA). The third uses GFZ's phase delay and the official GFZ FSI processor to provide FSI amplitude information. The fourth stream is processed in-house:

GFZ operational data: data as provided by GFZ's operational processing (Version 5), based on GFZ phase delay data (Version 2). This data is processed using FSI but does not provide information on the amplitude. It is available at:
http://isdc.gfz-potsdam.de/champ/

CDAAC operational data: data as provided by CDAAC's operational processing (Dec 2005). This data does not provide information on FSI amplitude. It is available at:
http://cosmic-io.cosmic.ucar.edu/cdaac/index.html

GFZ processed data: data generated from phase delay files, also providing information on FSI amplitude.

Met Office processed data: data processed at the Met Office, using GFZ-provided phase delay data. This data uses no FSI processing, it is only used to obtain information on fly-wheeling.

The first data stream is described in [27, 24], although it will soon be updated to Version 6 with a modified FSI and single differencing, leading to better temperatures and geopotentials. The second one is documented in [8] and uses an independently generated set of phase delays; recent occultations already use single differencing and the full dataset will be updated soon. The third stream is partly generated at GFZ and partly within this analysis, using Georg Beyerle's (GFZ, Potsdam) independent FSI processor based on MATLAB [26] and it also uses GFZ phase delay data (Version 2). It deviates slightly from the GFZ operational data since different quality control procedures are used. The fourth stream was processed by Christian Marquardt (Met Office, Exeter).

Most data are available from the start of the mission in May 2001 up to June 2005, in total about 200,000 profiles. The horizontal data coverage is plotted in Figure 1, showing the number of profiles per 4° latitude/longitude box. It clearly shows that the coverage of the CHAMP instrument is not uniform, especially when considering that the size of a latitude longitude box varies from almost 200,000 km^2 at the Equator and about 140,000 km^2 near mid-latitudes to about 35,000 km^2 near the poles. Thus a uniform distribution would show

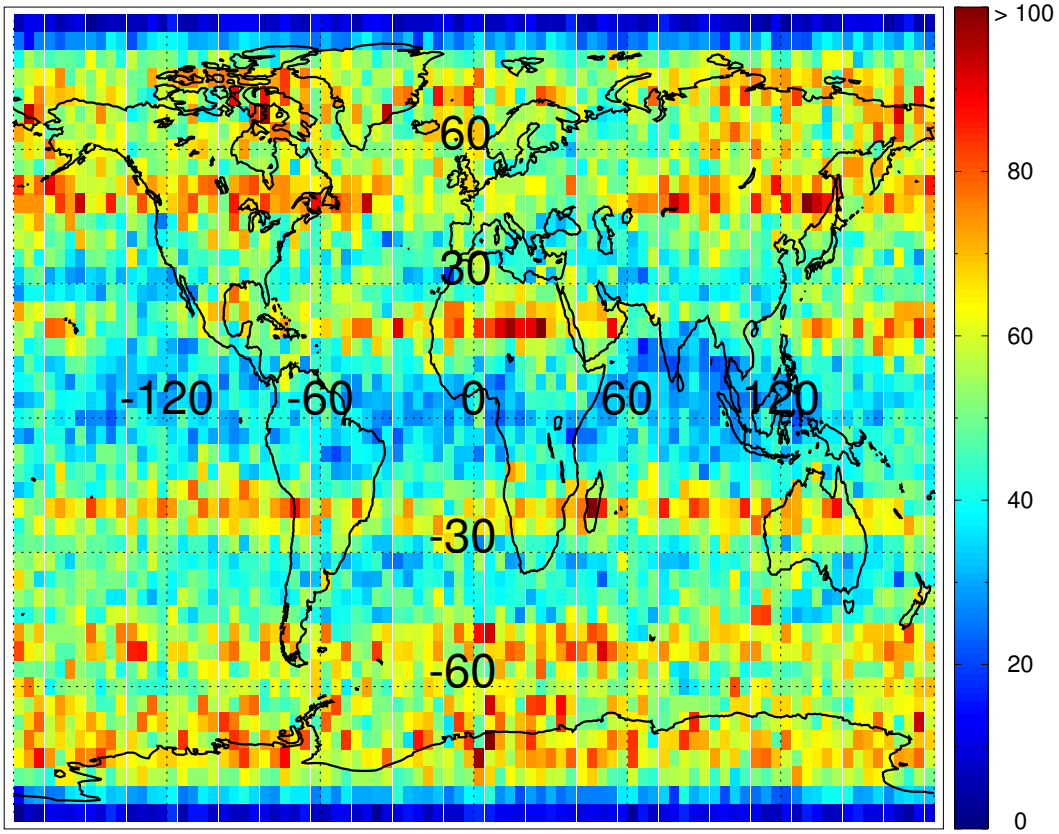

Figure 1: Number or profiles per 4° latitude longitude box. GFZ operational data, about 200,000 profiles.

about 6 times more profiles near the poles. The actual coverage is partly caused by the CHAMP orbit and partly by the GPS satellite orbit characteristics.

The horizontal coverage with respect to different seasons and the four-daily analysis times available in the ECMWF ERA 40 data is shown in Figures 2 and 3. The seasonal coverage for the months DJF, MAM, JJA, SON is 48,227, 56,663, 51,087, 47,639 occultations. The coverage with respect to universal times 00 UT, 06 UT, 12 UT, 18 UT is 51,236, 51,025, 51,240, 50,115 occultations. The closest universal time to the CHAMP observation time was used to sort occultations. Hence coverage between different seasons and universal times never varies by more than 20 %. Both plots show that the CHAMP instrumental coverage is not homogeneous which has potential implications for climate change observations when using a single radio occultation instrument.

The vertical coverage is partly determined by the noise on the measurement[1]. At higher altitudes, the actual bending is too small to be separated from the noise — this usually happens around 40 km. At lower altitudes, the lower signal amplitude together with noise leads to tracking loss of the GPS signal. The instrument's signal-to-noise ratios (SNR) can also be expressed as signal carrier-to-noise density ratio (SCN) in [dB Hz], where the following

[1]The SNR of the CHAMP observations determines the altitude where tracking is lost to some extent. Improved receivers will thus penetrate further down into the atmosphere; for a more detailed study refer to [3, 21].

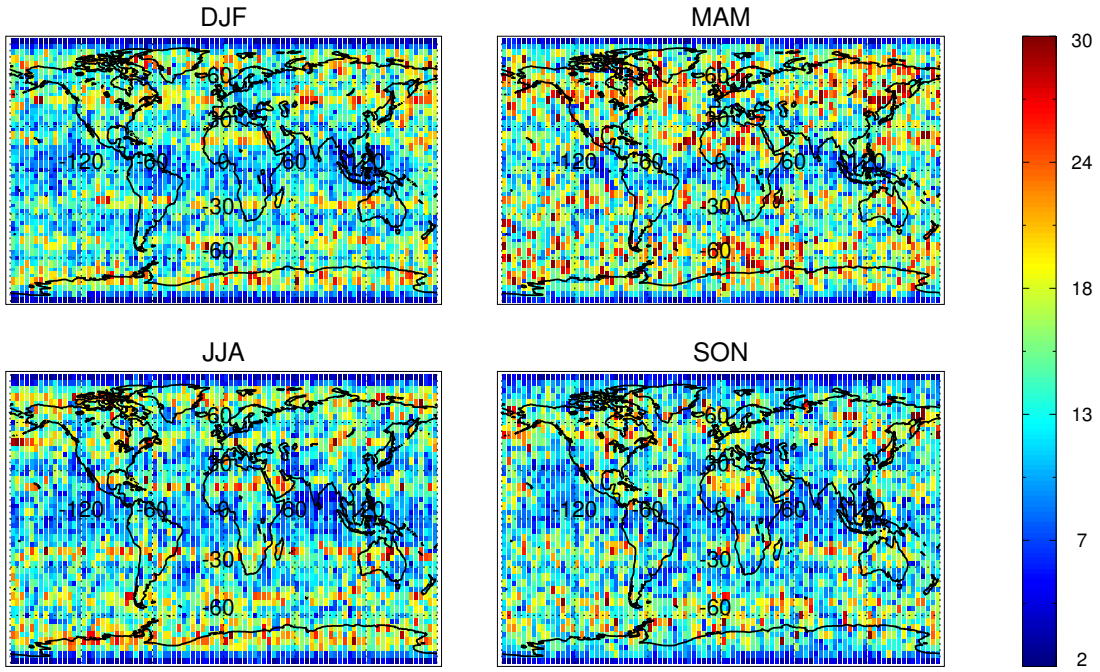

Figure 2: Number or profiles per 4° latitude/longitude box for different seasons. GFZ operational data (about 200,000 profiles).

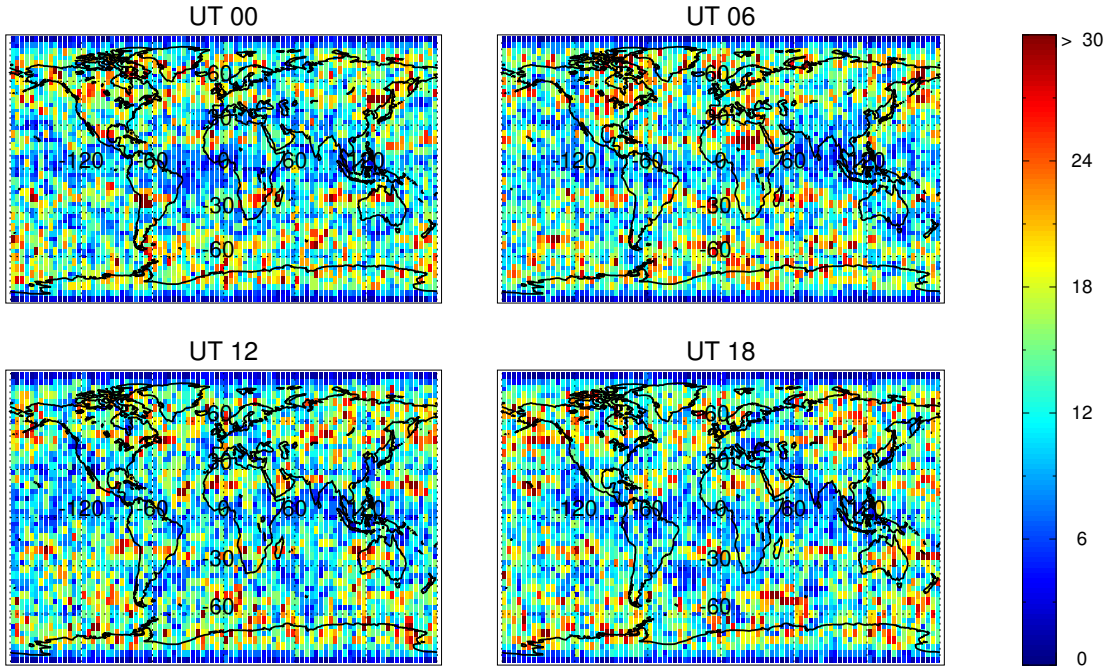

Figure 3: Number or profiles per 4° latitude/longitude box for different universal times. GFZ operational data (about 200,000 profiles).

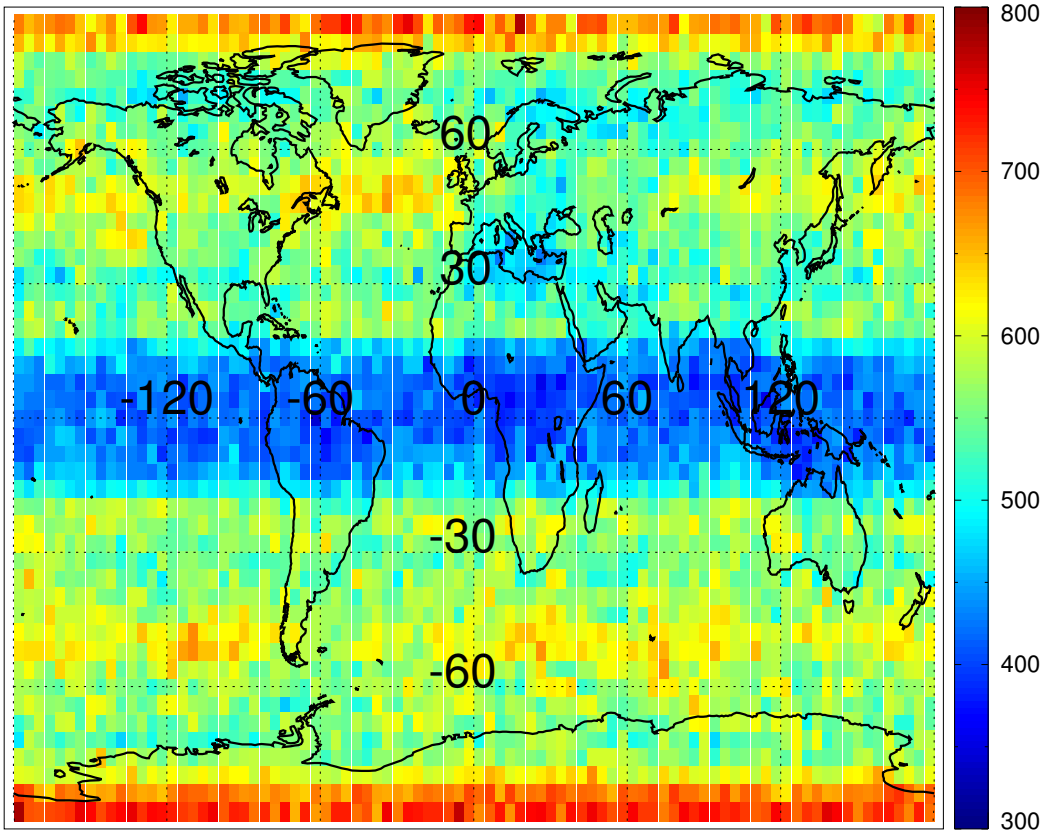

Figure 4: Mean signal-to-noise ratio of CHAMP observations, data is averaged over 4° latitude/longitude boxes. GFZ operational data (about 200,000 profiles).

formula applies:

$$SNR = \sqrt{2 * T * 10^{SCN/10}} \tag{1}$$

with the integration time T (where 1 s is used for the CHAMP BlackJack receiver SNR) [12].

Mean SNR values as derived from given GFZ CHAMP data at 40 km are presented in Figure 4, averaged over 4° latitude/longitude boxes. Tropical occultations clearly show a lower SNR than polar ones, caused by the geometry of the observation. Thus, tropical observations will generally loose tracking higher up in the atmosphere, caused by the geometry and the high concentration and variability of water vapour (for further information please refer to Section 5).

As mentioned above, radio occultation provides profiles of temperature, pressure and water vapour. But the measurement does not scan the atmosphere vertically, instead the tangent point track shows a horizontal displacement which is partly caused by the varying geometry of the observation and partly by the impact of the atmosphere. Figure 5 shows the mean horizontal displacement of the tangent point starting from the operational upper GFZ CHAMP altitude of 35 km. In this analysis, as well as in all presented latitude band separations shown in this report, occultations are divided by latitude θ into three different bands: polar ($|\theta| \geq 60°$), mid-latitude ($30° \leq |\theta| < 60°$), tropical ($|\theta| < 30°$).

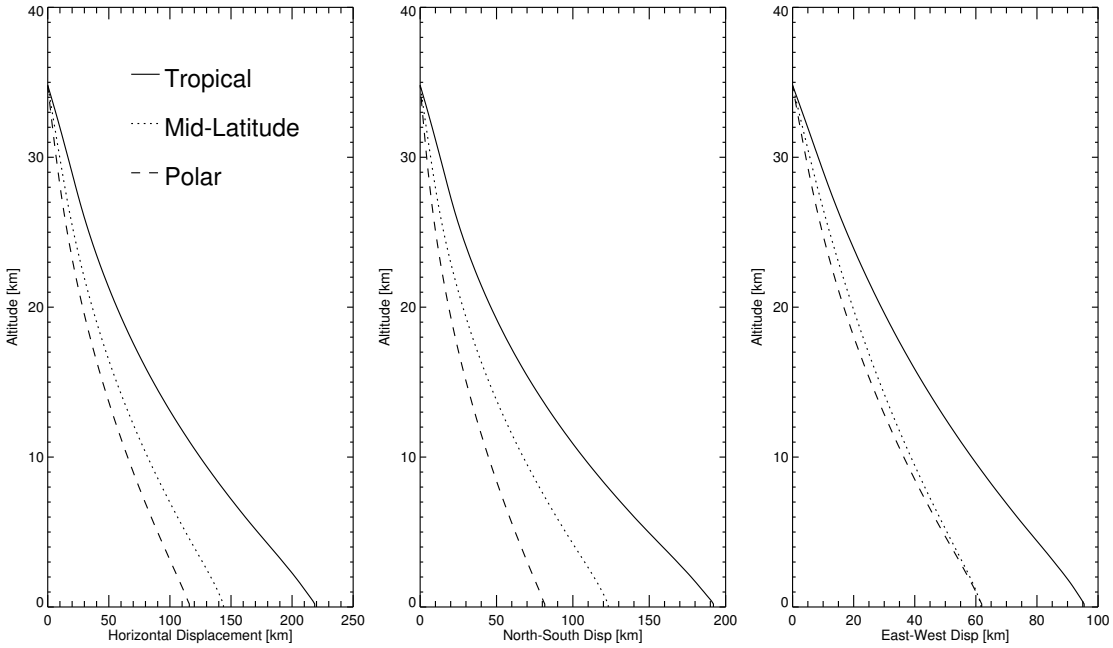

Figure 5: Mean horizontal displacement of CHAMP tangent point for different latitude bands. Left: total; Middle: along North – South axis; Right: along East – West axis. GFZ operational data (about 5,000 randomly selected profiles).

The main horizontal displacement is present at the lower range of the scan, thus when using vertical profiles from e.g. ECMWF fields for validation, a tangent point weighted towards the lower altitudes should be used. Figure 5 also shows that the main displacement is along the North–South axis, since the CHAMP satellite moves in this general direction and observes occultations looking aft. Possible consequences of this for validation are discussed in the next section.

4 ECMWF Background used

For validation purposes, this work uses ECMWF ERA 40 or ERA 40–like global atmospheric fields [19]. ERA 40 is a reanalysis project at ECMWF that covers the period of mid-1957 to 2001. Data is available on a 1.5° latitude/longitude grid. (Data not covered in the original ERA 40 project is taken from ECMWF operational analysis.) It provides 60 vertical levels, with about 18 levels between 0 km and 3 km; in the stratosphere the resolution is generally > 1 km. Data is available at analysis times of 00 UT, 06 UT, 12 UT, and 18 UT.

The actual location of the extracted validation profiles was taken from the available CHAMP tangent point track (GFZ operational data). As mentioned earlier, tangent points show a horizontal displacement of more than 100 km over the lowest 35 km of the scan (Figure 5). Additionally, the main horizontal variability is larger in the lower part of the atmosphere, compared to the upper altitudes. Thus ECMWF validation profiles should not be extracted at the mean tangent point, but weighted towards lower altitudes.

ECMWF validation profiles used here are:

- extracted at a weighted location, representing the mean of the lowest 20 km of the scan.
- extracted at the nearest analysis time.

Implication of these assumptions are discussed below.

Extracting ECMWF profiles along the tangent point would remove deviations caused by the horizontal displacement. This approach was not taken here since it will lead to validation profiles that are not hydrostatic. ECMWF fields are hydrostatic in the vertical and the hydrostatic equation is generally applied during the variational assimilation [6, 14, 15]. A pressure profile that follows the tangent point movement can deviate from a hydrostatic profile by up to 1 % [20].

An analysis of the horizontal variability in the ECMWF fields is shown in Figure 6. It shows the mean and standard deviation between an ECMWF profile extracted at the weighted location, and at the location of the lowest scan altitude, separated for refractivity, temperature, and water vapour pressure.

The highest standard deviation for refractivity is present at lower altitudes where it can reach 2 % at tropical latitudes. It should be noted that no bias is introduced in the refractivity profiles when using a weighted tangent point or one at the lowest scan altitude. For temperature, the standard deviation is generally below 1 K, almost independent of latitude or altitude. Water vapour shows relatively large standard deviations with a maximum around 5 km. Water vapour leads to the large standard deviations in refractivity at low altitudes, although the impact of water vapour on refractivity decreases with altitude, thus leading to the maximum around 2 km in refractivity. The found water vapour bias should be treated with caution, it varies when analysing different subsets of the data. A set of 5000 profiles might not be sufficient to draw a conclusion. These plots should be analyzed further to find an optimum location for the generation of a background profile in a variational assimilation that is closest to the expected retrieved profiles of water vapour and temperature.

Extracting ECMWF validation profiles and interpolating between the available analysis times to the measurement time would remove deviations caused by diurnal effects. This is also not performed over here to avoid the generation of non-hydrostatic profiles. An analysis of this assumption on the ECMWF validation profiles is shown in Figure 7. Here, the mean and standard deviation between a vertical ECMWF profile extracted at the weighted location and one that is interpolated linearly to the actual time of the measurement is shown (also based on weighted location profiles).

The standard deviations for refractivity at tropical latitudes are lower than the ones found for the lowest scan point (Figure 6) but are otherwise fairly similar for all latitude bands. The variations at low altitudes are again caused by the water vapour variability between different analysis times. Again, no bias is introduced by using a weighted profile at the nearest ECMWF analysis time over one that is interpolated in time. Temperature standard deviations increase with altitude caused by the diurnal cycle present in the mid- to upper-stratosphere. Hence a time interpolation should be performed to increase the background quality in a variational assimilation approach when retrieving stratospheric temperatures. For the found water vapour bias, the set of 5000 profiles might not be sufficient to draw a conclusion.

Figure 8 shows a comparison between CHAMP refractivity profiles and the three different ways to generate a validation profile. A time interpolated profile shows similar deviations

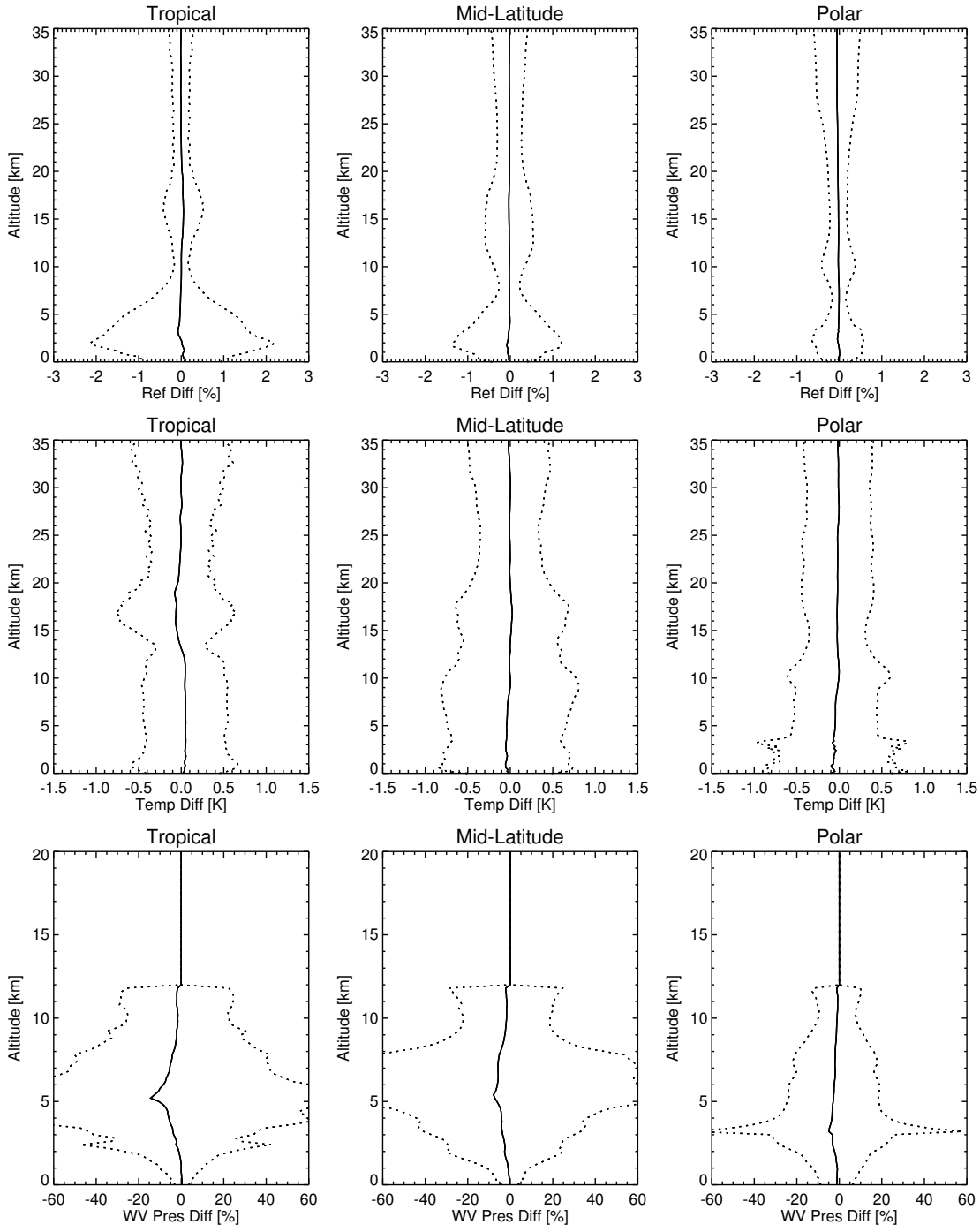

Figure 6: Mean (solid) and standard deviation (dotted) between an ECMWF profile extracted at the weighted location and one at the tangent point of the lowest scan altitude, separated by latitude band. Shown are refractivity (top), temperature (middle), and water vapour pressure (bottom). Location from GFZ operational data (about 5,000 randomly selected profiles).

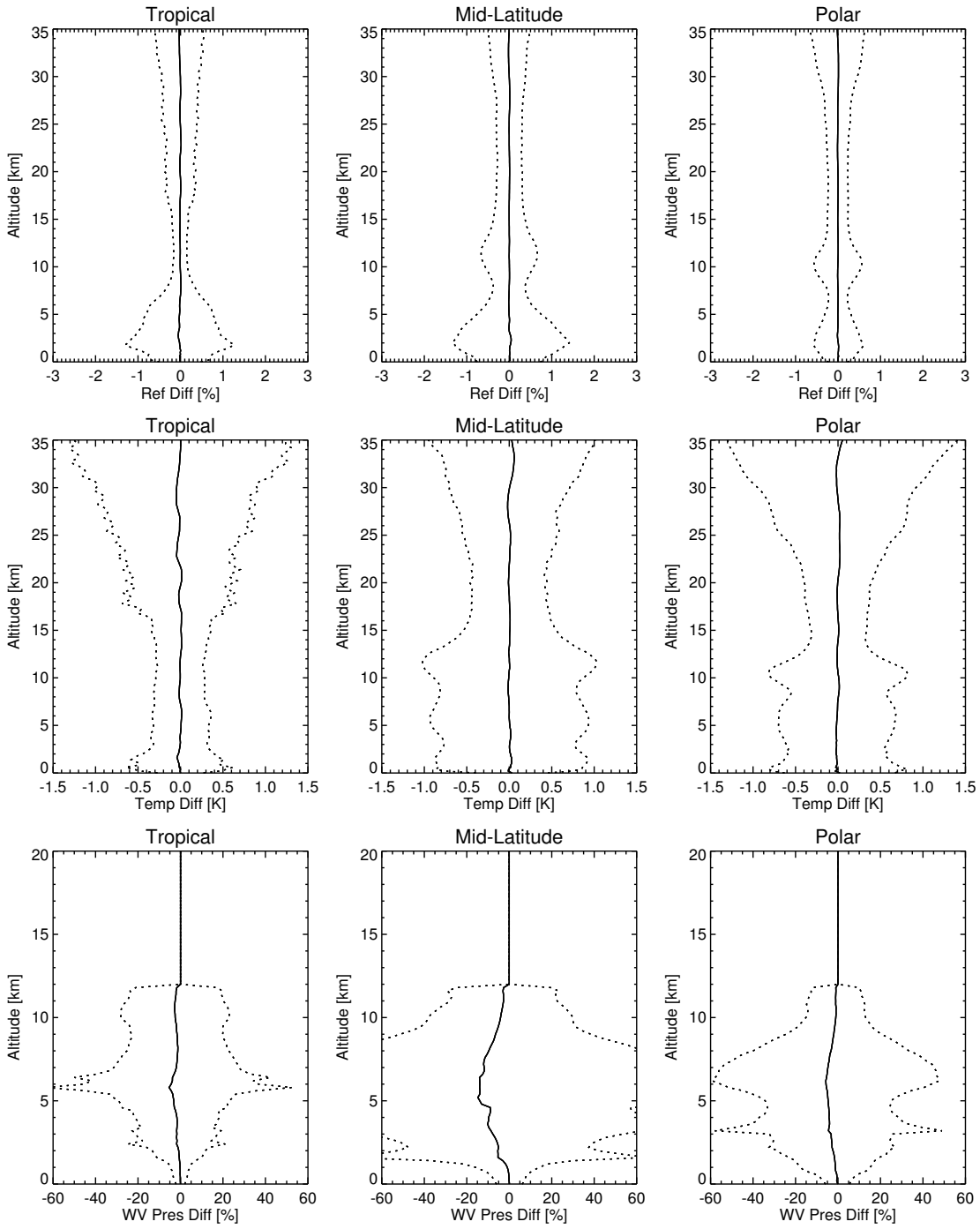

Figure 7: Mean (solid) and standard deviation (dotted) between an ECMWF profile extracted at the weighted location and one for the interpolated measurement time. Otherwise as Figure 6.

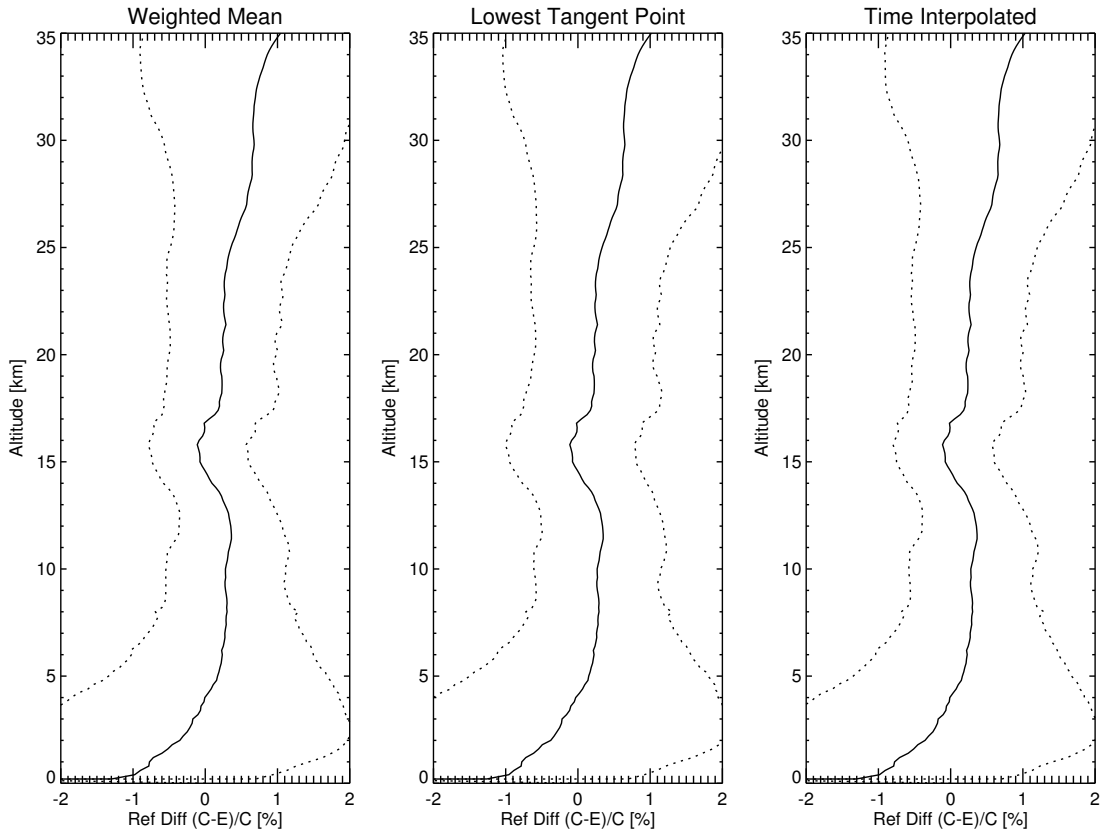

Figure 8: Mean and standard deviation between CHAMP occultations and corresponding ECMWF validation refractivity profiles. Left: weighted tangent point; Middle: lowest tangent point; Right: time interpolated. GFZ operational data (about 5,000 randomly selected profiles).

as the weighted one, the largest deviations are found for the lowest tangent point. It is thus possible to use a weighted tangent point for validation purposes. Biases are, as mentioned above, similar for all three validation profiles. Note also that the deviations found at higher altitudes in Figure 6 and 7 are only a fraction of the deviations found here; deviations at lower altitudes can have a similar magnitude.

5 FSI Amplitude Analysis

The FSI amplitude is used at GFZ (Potsdam) to determine the lowest sampled altitude of the CHAMP radio occultation instrument [27]. Hence it has characteristics similar to a signal-to-noise ratio. Typical normalized FSI amplitudes are shown in Figure 9 for an altitude of 7 km. The altitudes used here are with respect to the Earth surface, thus a 7 km altitude above land is not necessarily close to a 7 km altitude above the sea. Altitudes are derived from CHAMP impact parametres using ECMWF validation profiles. Since the amplitude itself is very variable, the mean over a 1 km wide vertical interval centered at 7 km was used to generate the plot.

The plot clearly shows the impact of the highly variable water vapour around the Intertropical

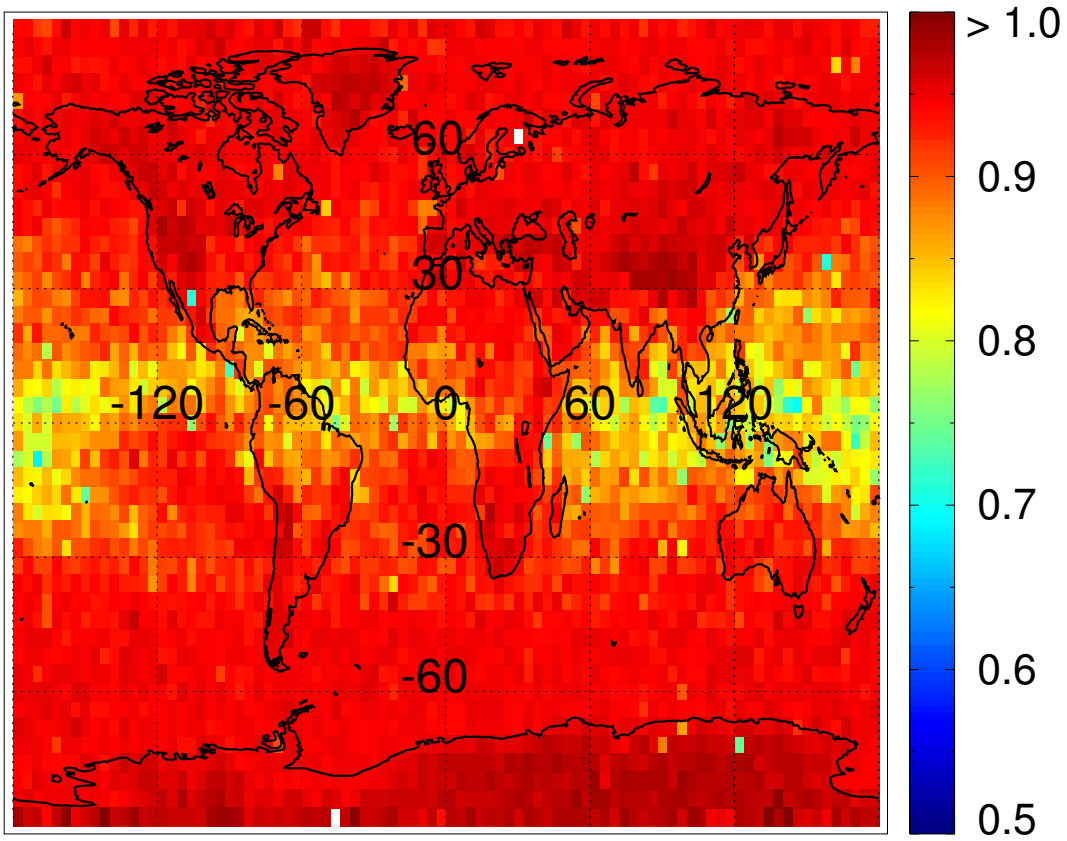

Figure 9: Mean FSI amplitude at 7 km above the earth surface. Data is averaged over 4° latitude/longitude boxes. Amplitudes are normalized with respect to the 10 km value, values higher than 1 are caused by strong amplitude fluctuations at lower altitudes. GFZ processed data (about 200,000 profiles).

Convergence and South Pacific Convergence Zones (ITCZ and SPCZ) on the data coverage where the FSI amplitude is reduced by more than 20 % inbetween the altitudes 10 km and 7 km. It also shows that the SNR (Figure 4) is not the only factor determining the FSI amplitude and thus the lowest scan altitude reached. A seasonally separated plot of this data also shows the impact of seasons on the FSI amplitude, thus lower FSI amplitudes are found during Northern Hemisphere summer than winter at northern latitudes (not shown).

While Figure 1 shows the number of profiles in a latitude longitude box, it does not provide information on the vertical coverage of the occultations. The number of operational CHAMP profiles that actually terminate above 4 km altitude is shown in Figure 10. It also shows the dominant influence of the ITCZ and SPCZ.

6 FSI Amplitude Variability Analysis

The CHAMP FSI amplitudes were analyzed for their altitude dependence within the troposphere. Amplitudes were first normalized to the maximum value found in the lowest 20 km so that they do not exceed a value of 1.0. These maximum FSI amplitude values are generally found at low altitudes since the FSI amplitude can be very noisy. Amplitudes were

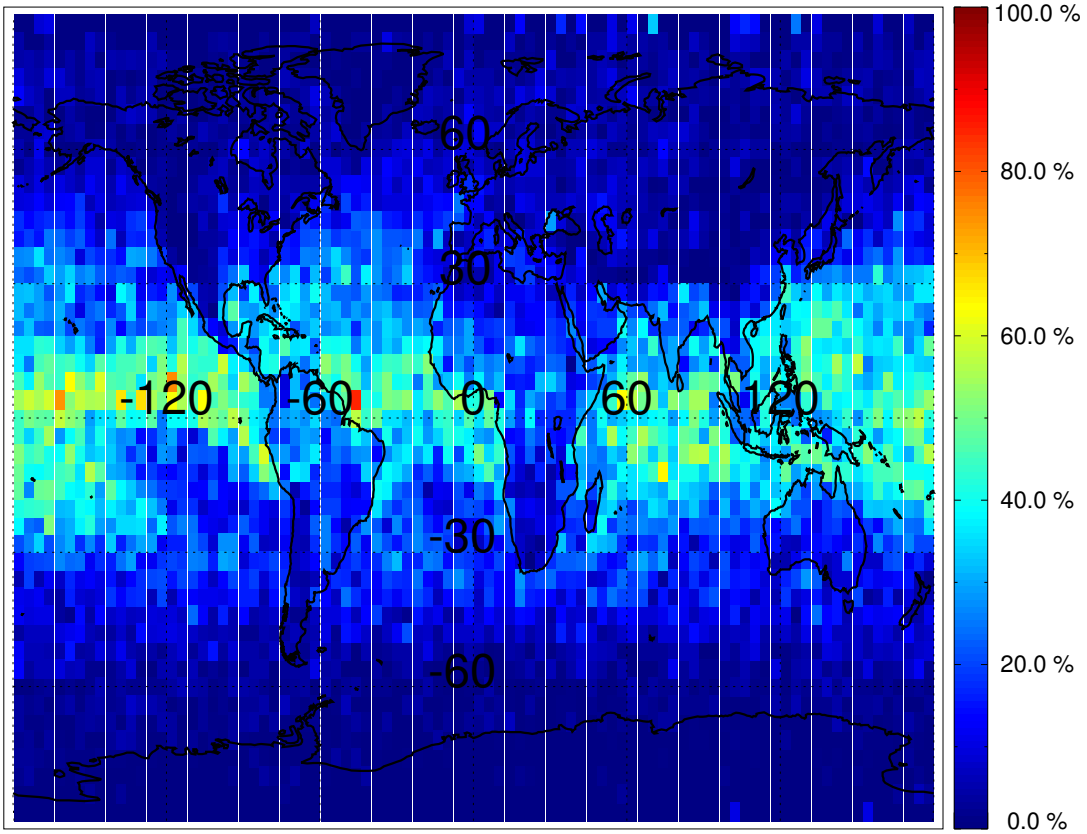

Figure 10: CHAMP percentage of profiles terminating above 4 km altitude above the earth surface. Data is averaged over 4° latitude/longitude boxes. GFZ operational data (about 200,000 profiles).

additionally smoothed with a 0.5 km boxcar average to remove pure noise effects. Note that this normalization results in a somewhat un-physical behavior of the FSI amplitude in the stratosphere and upper troposphere. Here, absorption and other effects are small, thus all normalized amplitudes should be 1 here.

The mean FSI amplitude values for the 3 different latitude bands are shown in Figure 11. Altitudes have been calculated from impact parametres using ECMWF validation profiles. The feature at 20 km altitude is caused by the normalization process.

Tropical occultations show the lowest mean values at higher altitudes, caused by the above-mentioned normalization, since strong FSI amplitude fluctuations are present at lower altitudes. Otherwise, independently of latitude band or land sea location, all occultations show a reduction in mean FSI amplitude from about 8 km.

The variations of the FSI amplitude over altitude were calculated by dividing the found standard deviation of a certain set of occultations at that altitude by the mean over these occultations. The results are shown in Figures 12. Variations are very similar for all latitudes and do not differ significantly for land- or sea-based occultations. Strong variability starts at about 10 km in the tropics. Also visible is the slightly higher altitude where tropical occultations are affected when observed over sea. This is also evident in polar sea-based observations. The reduction in variability at low altitudes in e.g. tropical occultations is caused by tracking loss when variability is high. Thus, at lower altitudes, observations are

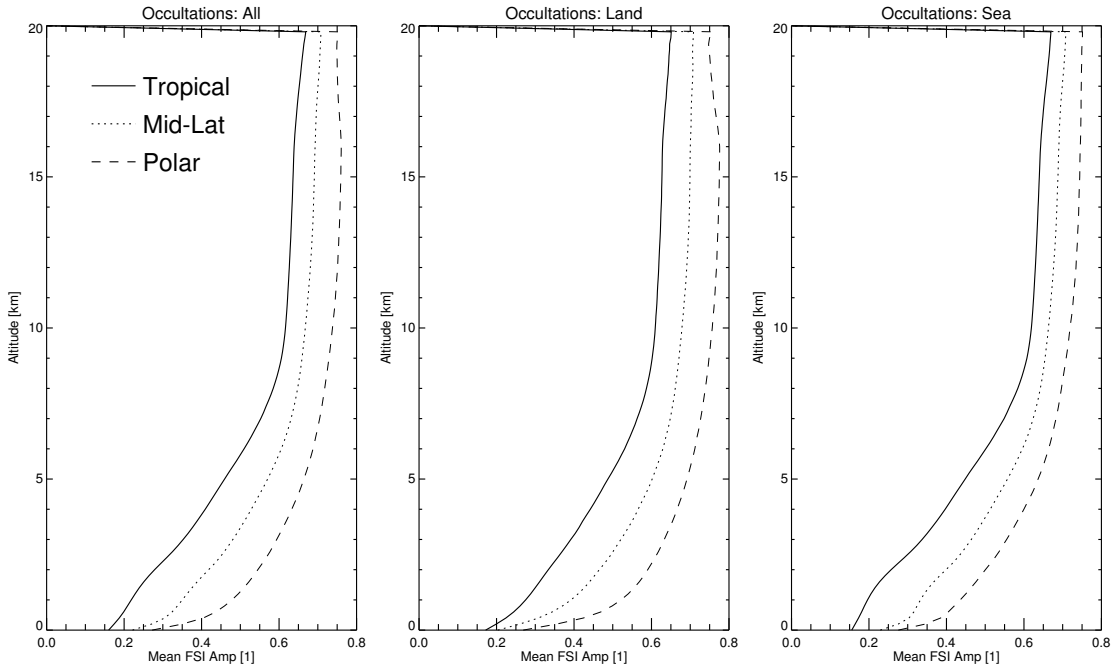

Figure 11: CHAMP FSI mean amplitude separated by latitude band and land/sea events. GFZ processed data (about 200,000 profiles).

biased towards ”calm” atmospheric conditions.

7 FSI Amplitude Cutoff Analysis

The CHAMP operational processing stops when the normalized, smoothed FSI amplitude drops below a value of 0.5. The threshold is essentially a trade-off between the profile quality (assessed generally in comparison to ECMWF profiles) and the number of profiles penetrating a certain altitude. The impact on the refractivity standard deviation and bias with respect to ECMWF validation profiles has been assessed for FSI amplitude thresholds of 0.3, 0.5 (operational setting), and 0.7 for a limited period. In total, 4,730 profiles from January 2003 have been processed. The profile locations are shown in Figure 13. It is already evident from this figure that the majority of profiles terminate close to the surface in the drier, high latitude regions. Tropical occultations more frequently terminate higher up in the atmosphere.

Bias and standard deviations are shown in Figure 14. Also shown is the normalized number of profiles at each altitude level. Altitudes here are with respect to the geoid (mean sea level). The FSI threshold setting influences the data quality as can be seen from the standard deviations. A higher threshold also filters out occultations that lead to a bias in the obtained refractivity profiles at lower altitudes. But it is also evident from this figure that higher thresholds will significantly reduce the number of profiles in the lower troposphere, e.g. the 50 % level is about 2 km higher for a higher setting compared to the operational one.

Figure 15 shows the refractivity standard deviations for different latitude bands. The major impact on the quality is found at tropical latitudes, where high amounts of water vapour are

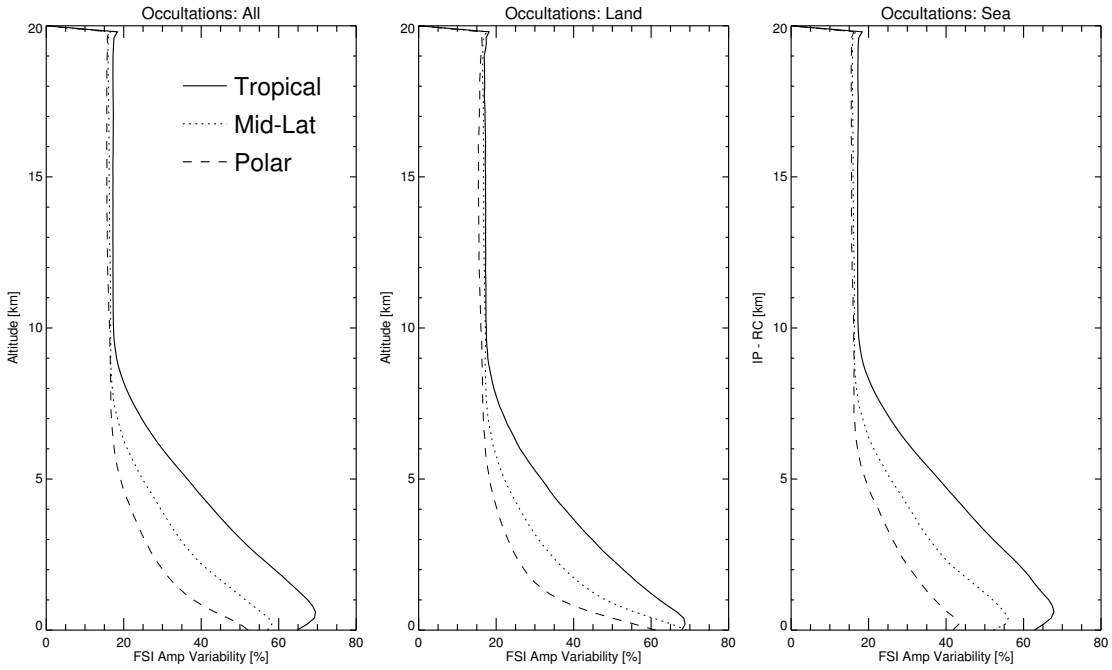

Figure 12: CHAMP FSI amplitude variations separated by latitude band and land/sea events. GFZ processed data (about 200,000 occultations).

present. This is also evident from the figures in Section 6.

For completeness, Figure 16 shows the refractivity standard deviations separated by land- and sea-based occultations for the operational threshold setting of 0.5. The fact that the bias looks slightly better for sea-based events at all altitudes could point to an inconsistency with the altitude referencing between CHAMP and ECMWF data used here. Other factors responsible for the different bias behavior are the impact of critical refraction and the deviation from a spherical symmetry which could differ between land and sea events. The other FSI thresholds also show very similar results.

For a further analysis on the impact of the receiver tracking on the retrieved refractivity profiles refer to [3].

8 Fly Wheeling Analysis

In earlier radio occultation receiver software implementations, a measurement would be terminated once the tracking was lost, even if this only happened for a short period. More recent software implementations use so-called fly-wheeling to allow recovery after short interruptions in the tracking [5]. The altitude where fly-wheeling starts has been analyzed by processing GFZ phase delay data from the CHAMP instrument in-house for the years 2002 and 2003. The duration of fly-wheeling was calculated for different interruption intervals based on a 50 Hz sampling. Only the maximum altitude within a certain interruption interval enters this analysis, thus occultations can only enter once per interval. Figure 17 shows the results of this analysis for different latitude bands and land sea events. Fly-wheeling is given as a function of impact parametre. ECMWF validation profiles were used to convert impact

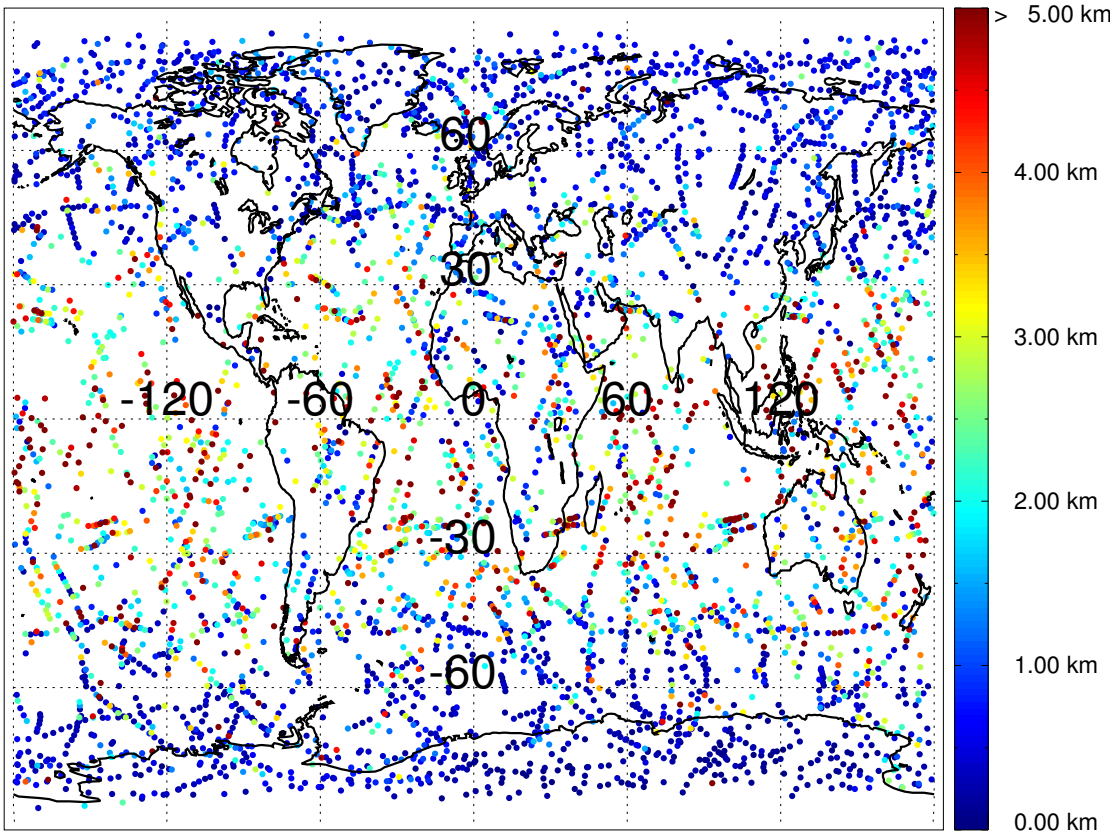

Figure 13: CHAMP profile locations used for FSI amplitude threshold assessment. The color code gives the lowest sampled altitude of the 0.5 operational FSI threshold setting with respect to the Earth surface. GFZ processed data from January 2003 (4,730 profiles).

parametres into altitudes for this plot. No topography correction has been performed, thus given altitudes are with respect to the geoid.

The method to determine fly-wheeling is described in [11]; it uses an approach similar to the one implemented on-board CHAMP. It is based on the L1 amplitude — the fly-wheeling flag is raised when an SNR value falls below a threshold of 50; it remains active for at least 3 samples (60 ms) and the flagging stops when a SNR value returns above a second threshold of 60.

A significant number of occultations show brief fly-wheeling even around 7 km in the tropics, as given by the maximum altitude. This is independent of land- or sea-based events. As mentioned above, each occultation only enters each interval once, thus about 40 % of all tropical occultations show fly-wheeling between 6 km and 8 km, an altitude already identified in a separate analysis of the FSI amplitude to show strong interruptions in the FSI amplitude [21]. Longer periods of fly-wheeling start to appear at lower altitudes; all extended periods of fly-wheeling show a large increase below 2 km. Sea-based tropical events show an increase in the number of fly-wheeling events with periods < 0.1 s at about 2 km, possibly caused by the top of the planetary boundary layer [22].

The other latitude bands show that the maximum altitude where fly-wheeling first occurs decreases with the humidity in the atmosphere. For polar land-based events, all extended periods of fly-wheeling start to increase at around 4 km, while for sea based events a strong

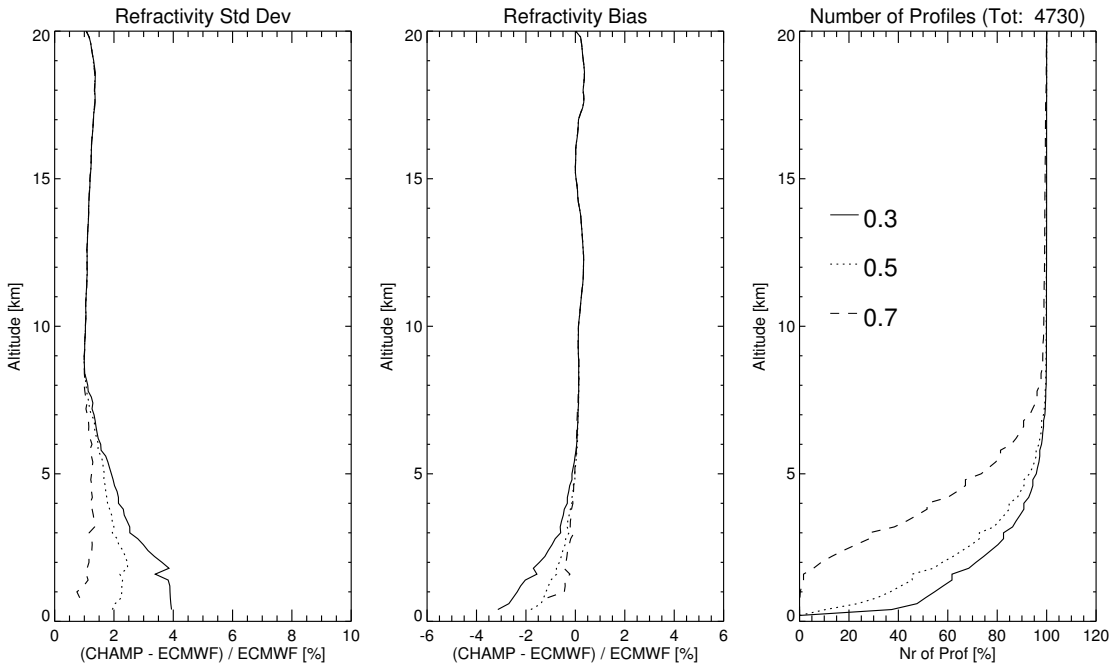

Figure 14: Global CHAMP standard deviation and bias with respect to ECMWF refractivity profiles for different FSI threshold settings. Normalized number of profiles on the right. GFZ processed data from January 2003 (4,730 profiles).

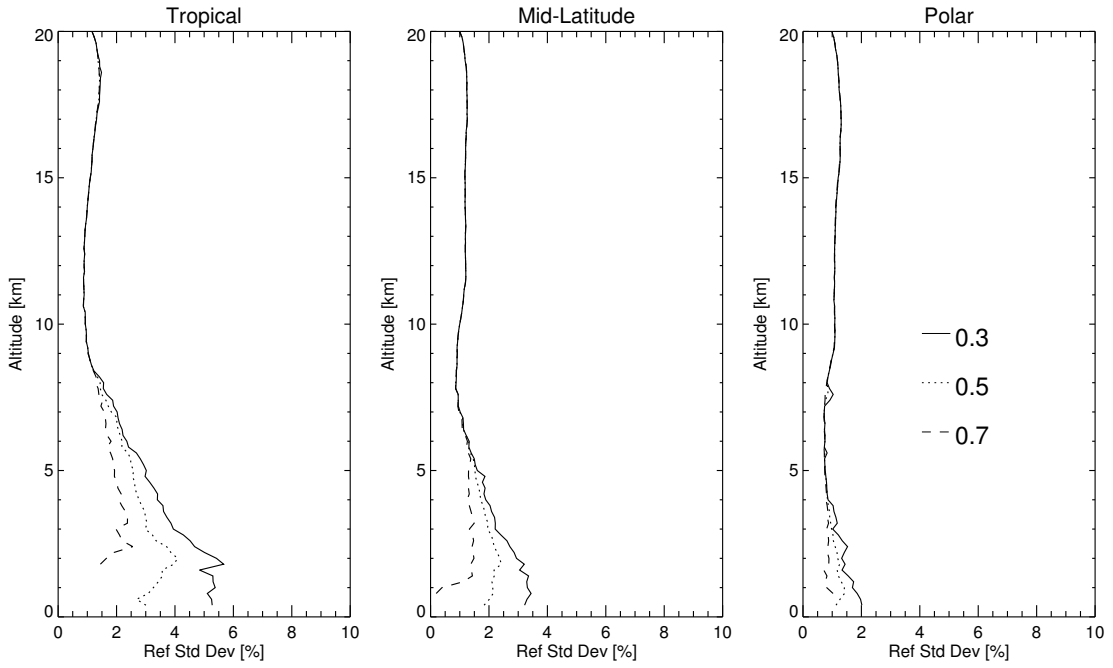

Figure 15: Latitudinal CHAMP standard deviation with respect to ECMWF refractivity profiles for different FSI threshold settings. GFZ processed data from January 2003 (4,730 profiles).

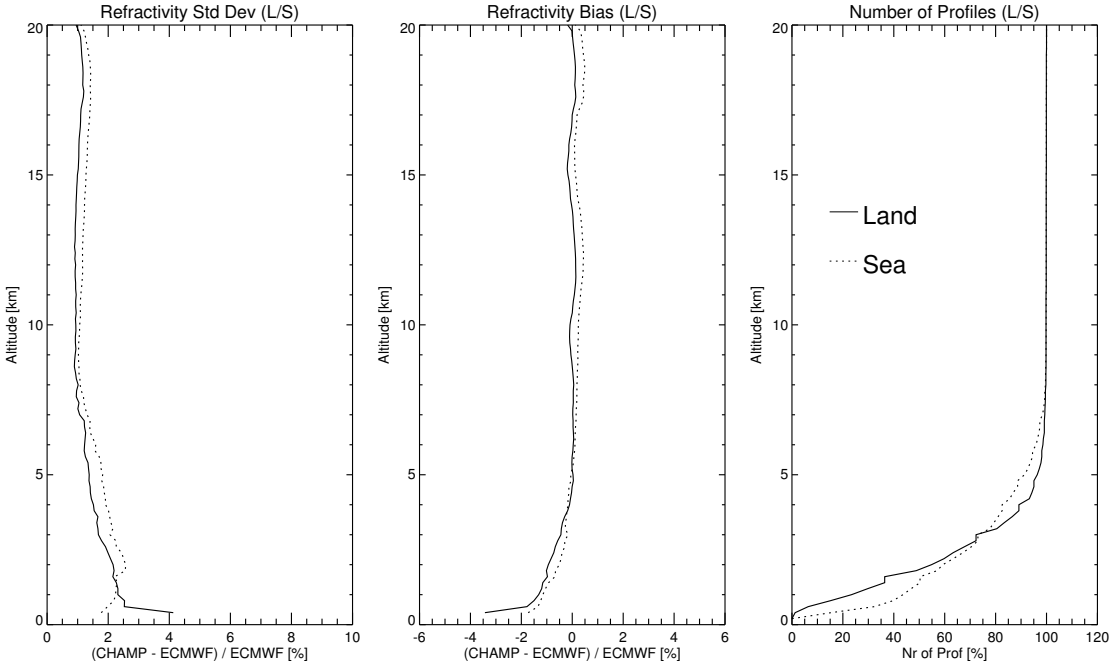

Figure 16: Land/Sea CHAMP standard deviation and bias with respect to ECMWF refractivity profiles for an FSI threshold settings of 0.5. Normalized number of profiles on the right. GFZ FSI processed data from January 2003 (4,730 profiles, 3,116 sea 1,614 land based).

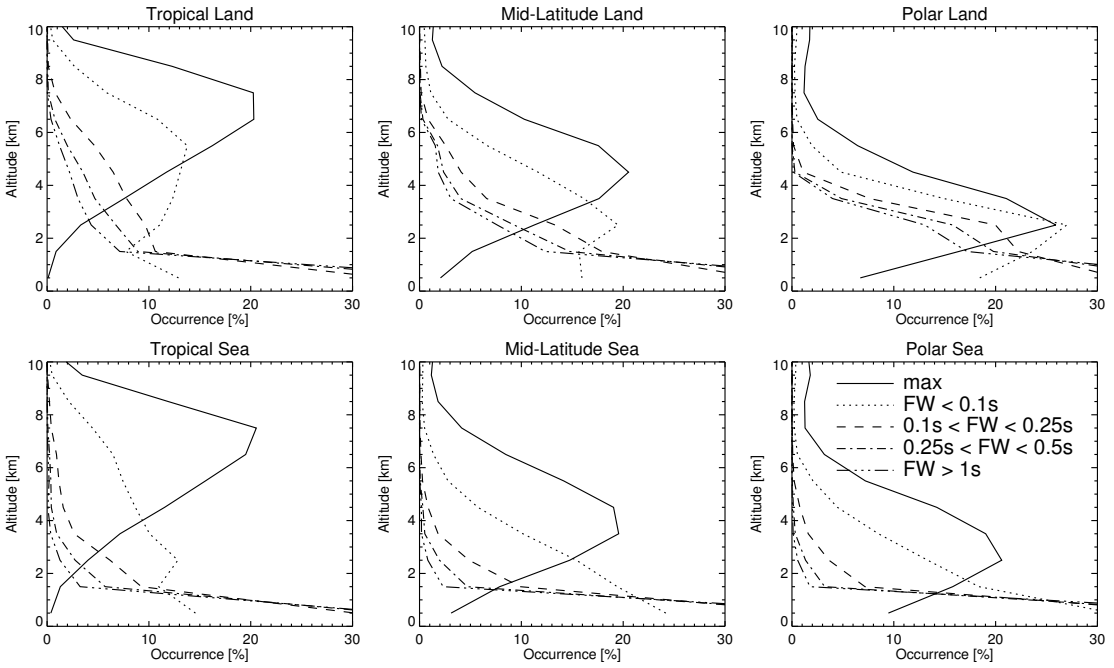

Figure 17: Percentage of CHAMP profiles showing different fly-wheeling intervals starting at a certain altitude, separated by latitude and land/sea events. Binsize 1 km. Met Office processed data (45,756 profiles, 30,129 sea 15,627 land based).

increase is found around 1.5 km. This is probably caused by the topography at polar latitudes.

A further analysis of fly-wheeling events (not shown) reveals that most of the extended fly-wheeling times (> 0.1 s) at higher altitudes are caused by topographic effects, e.g. the Himalayas or the Antarctic ice shelf. The general features of the FSI amplitude (Figure 9) can also be found in the fly-wheeling results, e.g. the ITCZ and SPCZ show up.

Fly-wheeling itself will be replace by open loop tracking in the near future, which should allow better recovery of occultation events affected by temporary tracking loss. Although the actual occultations affected will be similar to the ones shown over here. For data assimilation using fly-wheeling affected observation it is recommended to use this also as a quality control. However, the data set used over here could not be used to estimate a maximum time of fly-wheeling that would still be acceptable for assimilation since it does not apply the latest FSI processing and was mainly generated to analyse fly-wheeling occurrence.

9 Ground Station Analysis

The currently applied double differencing of the CHAMP processing [25] requires the simultaneous data from a reference satellite and a ground station. Often, an occultation has several ground stations available for processing, thus assuring redundancy in the network [25]. Here we analyze the refractivity profile quality by first sorting CHAMP operational FSI data by the ground station used for the differencing and then comparing them to the ECMWF validation profiles. This could provide information about whether a particular ground station affects the data quality.

Figure 18 shows the number of occultations per latitude/longitude box for different ground stations. The plots show that on the one hand some ground stations are primarily used for certain locations (e.g. NYA2 for most Northern latitudes), on the other hand they show that each ground station has a certain pattern, determined by the visibility of the ground station from the reference satellite.

The refractivity bias and standard deviation with respect to the ECMWF validation profiles is shown in Figure 19. Within each approximate latitude band, the standard deviation is used to sort the different ground stations. Sorting has been performed by integrating the standard deviation for each station over all altitudes and plotting the stations in this order where the highest integrated standard deviation appears first.

The bias plots show that biases are essentially independent of ground station up to about 20 km except for the stations GODE and CORD which show stronger biases. Above 20 km, ground stations seem to group into three different biases, in particular near the processing top of 35 km. This might be caused by the quality of ECMWF data for a particular location on the Earth.

The standard deviations also mostly agree for different ground stations, although there are some clear exceptions. Some of the outliers might be explained by the low number of occultations and thus the less reliable statistics (e.g. GODE, CORD), but BAN2 also shows larger standard deviations than other comparable stations and has a relatively large number of occultations. But it is also interesting to note that e.g. the stations GODE and CORD show large standard deviations, but low biases at high altitudes. One explanation would be the data quality at higher altitudes. If the data for these ground stations still has sufficient in-

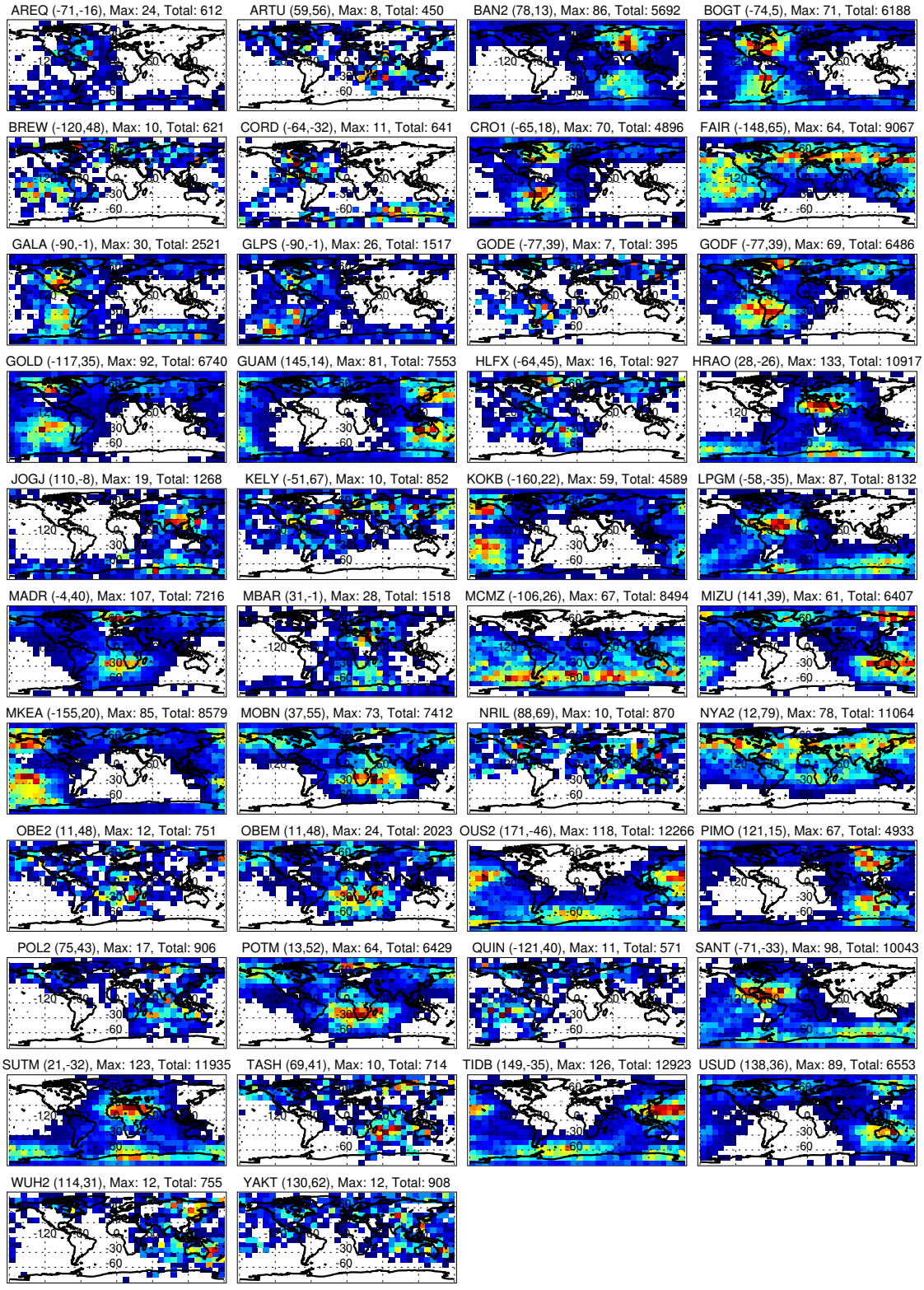

Figure 18: Number of profiles per 10° latitude longitude box for different ground stations. Ground station name is given in title, along with the longitude/latitude position in brackets. Color scale is from 1 occultation (blue) to maximum number (red) as given in title (white means no occultation found). The total number is also given. GFZ operational data (about 200,000 profiles).

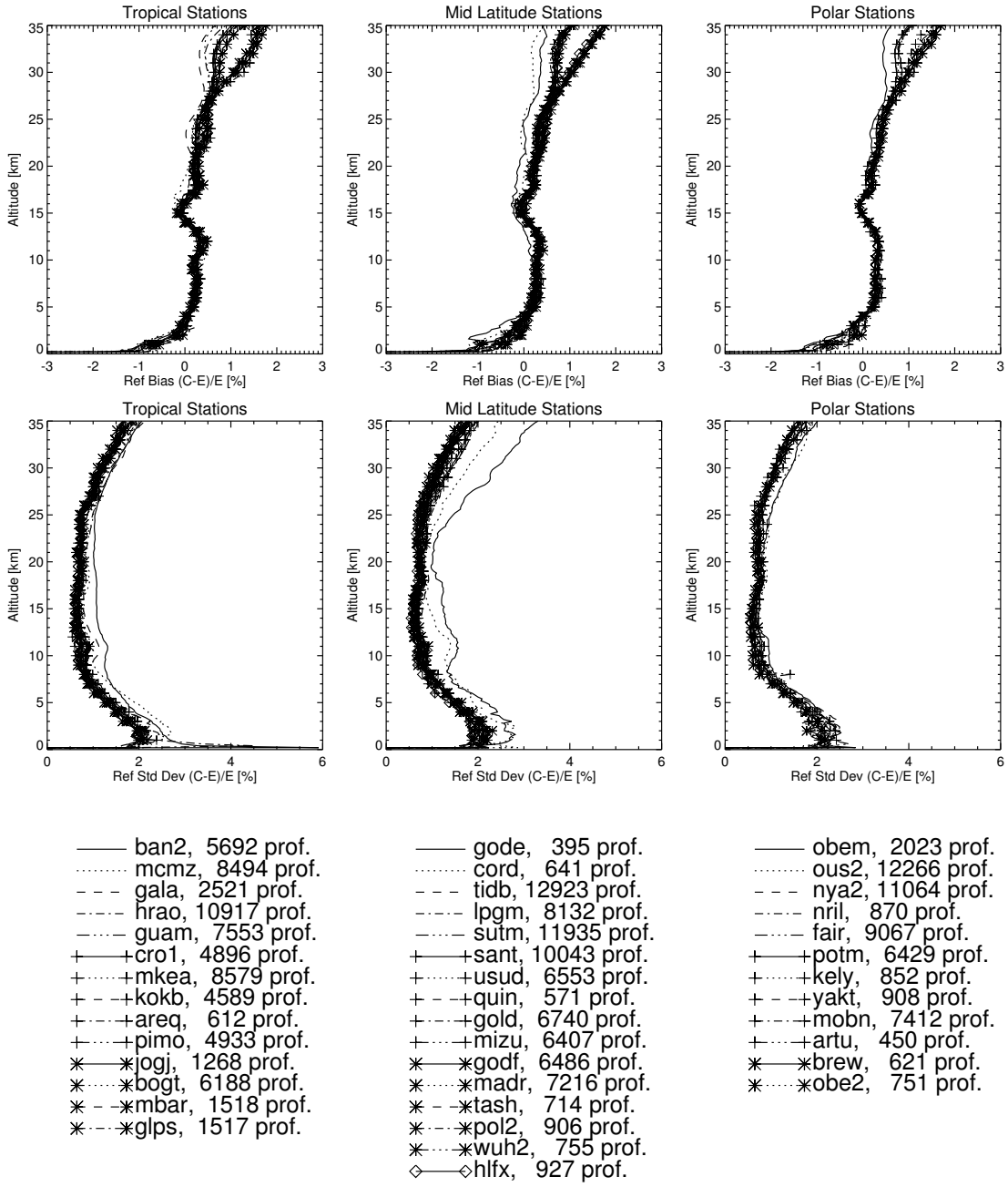

Figure 19: Refractivity bias (top) and standard deviation (middle) of CHAMP occultations with respect to ECMWF validation profiles separated by ground station. Ground stations are sorted into approximate latitude bands to have a similar number in each plot. GFZ operational data (about 200,000 profiles).

formation to extract refractivity at these altitudes, an increase in the standard deviation with respect to ECMWF would be observed, along with a lower bias than the other stations. This is supported by the fact that e.g. CORD has the highest mean SNR of all ground stations.

A further separation of the actual data into latitude bands has been performed to remove to some extent effects caused by the SNR pattern (different locations have different SNRs, see Figure 4) and effects caused by the quality of the available ECMWF data. The resulting plots (not shown) still shows some stations to be very different to the rest, in particular CORD and GODE. Whether this is caused by noise on the reference link, as discussed in [2] is not certain. Thus no clear conclusion can be drawn from these results presently.

It might be interesting to follow this up further and obtain radio occultation observations where each occultation is processed using different ground stations since the redundancy is usually above two [25]. This could provide an answer as to whether the results are caused by the ground station itself or are caused by the coverage of the station where for example stations observing occultations with lower ionospheric activity or primarily polar occultations would yield better results. Soon, GFZ will move to single-differencing with Version 6 and a further analysis of the new data might provide new insights.

10 GPS Satellite Analysis

An analysis similar to the one with respect to the ground station was also performed with respect to the occulting GPS satellite. Currently there are 29 active satellites, the oldest satellite in service is from Oct 1990, the newest from Sep 2005 (valid November 2005) [13]. Satellites are in six orbital planes (named A to F) with an altitude of approximately 20,000 km above the Earth's surface. Each orbital plane holds at least 4 satellites (numbered 1 to 4), although spare satellites are available which increase the total number of GPS satellites above the nominal constellation of 24. The orbital period is approximately 12 hours. Since the start of the CHAMP mission in 2001, seven new GPS satellites have been launched with PRNs 02, 16, 17, 19, 21, 22, 23 (GPS satellites are often identified by their Pseudo Random Number PRN) [13]. Hence, performing such an analysis over longer periods leads to the use of older and newer GPS satellites for one PRN since the PRN number are not unique with respect to a physical satellite. Once a satellite is decommissioned, the freed PRN is used by a new satellite. The PRN might also not refer to the same orbit plane with a new satellite.

Figure 20 shows the number of occultations per latitude/longitude box for different PRNs. The plots show that the actual orbit plane affects the coverage, caused by the GPS and the CHAMP satellite positions. Hence, similar patterns are found for the same orbit plane for some PRN numbers, although different patterns are also present, possibly caused by replacement of older satellites.

The refractivity bias and standard deviation with respect to ECMWF validation profiles is shown in Figure 21. Within each set, the standard deviation is used to sort the different GPS satellites.

The bias is very similar for most GPS satellites, although some show significant deviations, e.g. PRN 16 in the first set. This satellite is a more recent addition to the GPS constellation and the older satellite that was using PRN 16 was decommissioned before the CHAMP mission started and thus does not affect the results presented here. The second set shows

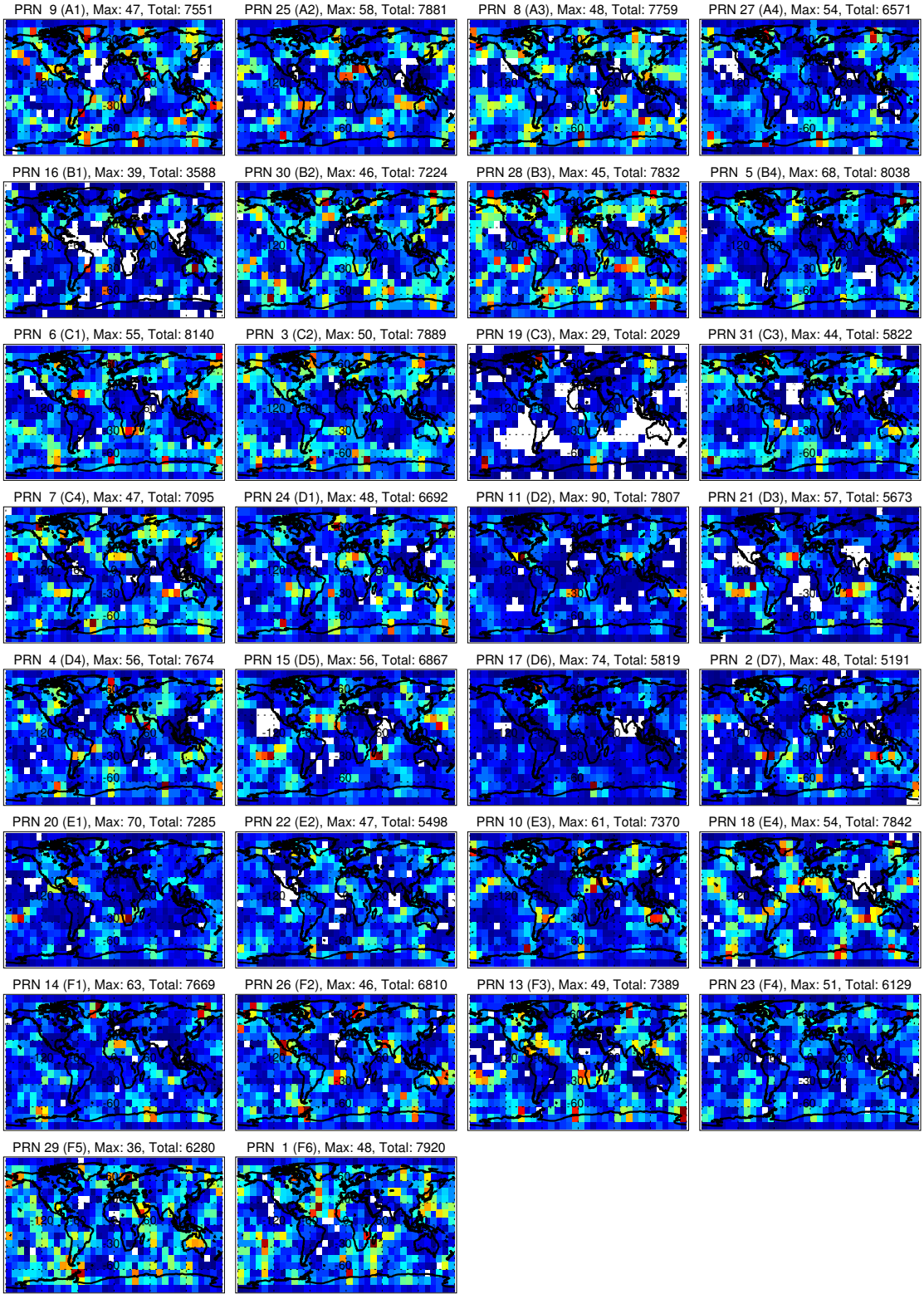

Figure 20: Number of profiles per 10° latitude/longitude box for different PRNs. PRN number is given in the title with the orbit plane in brackets. Color scale is from 1 occultation (blue) to maximum number (red) as given in the title (white means no occultation found). The total number is also given. GFZ operational data (about 200,000 profiles).

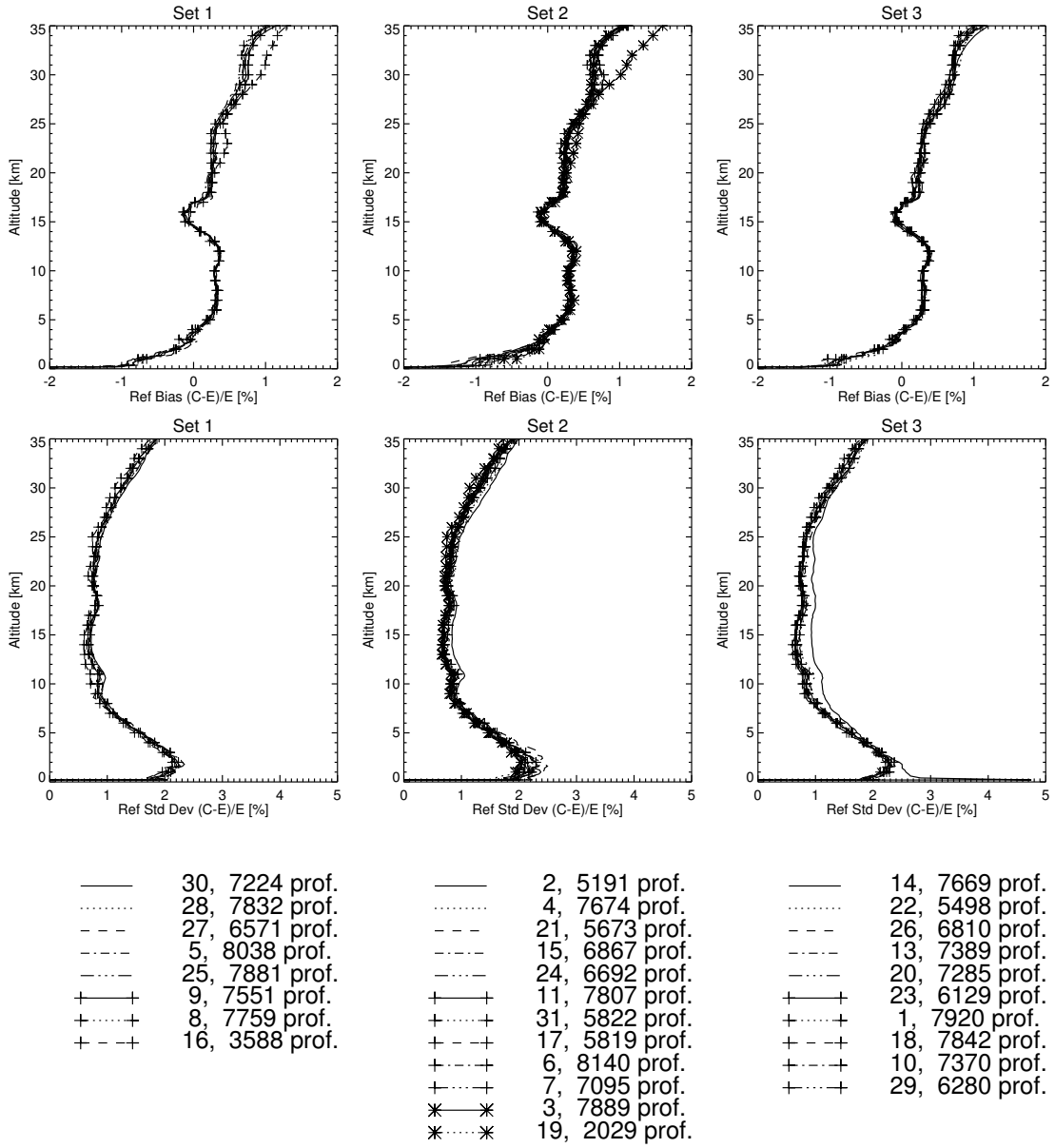

Figure 21: Refractivity bias (top) and standard deviation (middle) of CHAMP occultation with respect to ECMWF validation profile separated by PRN. PRNs are sorted into 3 sets of orbit planes. GFZ operational data (about 200,000 profiles).

GPS satellite 19 — also a recent addition to the constellation — to be significantly different. The old satellite using PRN 19 was decommissioned in September 2001 and thus contributes very few profiles to the overall statistics. In fact, a separate analysis of 2001 data shows that this satellite shows no significant difference from the other ones. The other later additions to the constellation do not show such a significantly different bias.

The standard deviations again single out different satellites more so than the bias plot. Whether this is caused by less noise on these occultations and thus less ECMWF information entering the retrieval process is not clear. An analysis of the SNR for the different satellites shows that the mean SNR is varying around 500 to 620 with no apparent correlation to the presented results.

Again, a simple separation into latitude bands still shows some PRNs very different from the rest. It is currently unclear why the PRNs differ. One possible explanation might be noise on the reference link as discussed in [2] where the actual ionospheric activity could affect the results. Although, this is more likely for the ground stations involved since they will primarily observe the reference link through a certain ionospheric location.

11 Processing Centre Analysis

Radio occultation has the unique feature that it works essentially without calibration and thus allows the combination of different instruments to develop a long term dataset for climate monitoring and benchmarking. Microwave or infrared instruments do not have this feature as they rely on calibration processes during operation to achieve their measurement accuracy. The calibration itself changes within the lifetime of an instrument and also between different instruments, thus the generation of long term datasets is problematic.

However, the generation of a long term radio occultation dataset for climate monitoring not only relies on a combination of different satellites, but data might also be processed at different centres. Several centres are providing data or are planning to provide data in the near future, e.g. GFZ (Potsdam, Germany), JPL (Pasadena, USA), UCAR (Boulder, USA), GRAS-SAF (Copenhagen, Denmark). This processing might introduce deviations in the derived atmospheric profiles that enter a validation, as for example discussed for the GRAS-SAF products in [10].

An early comparison of different processing centres (ROSE: Radio Occultation Sensor Evaluation) has been performed based on data from August 2002 for the processing centres GFZ, JPL and CDAAC [1]. This analysis did not include recent FSI processing, the applied processing is different from the operational ones, and the set of occultations was slightly different for each processing centre. The next step within the ROSE campaign is currently being processed where FSI data is used; first results were presented at the EGU [23].

A comparison of CHAMP and SAC-C measurements performed in [5] used the same processing centre for both satellites and thus provides no answer to the impact of the centre. Here we present a preliminary analysis of two processing centres (GFZ, Potsdam, Germany and CDAAC, Boulder, USA) using the same set of CHAMP occultations. We adopt an external user approach where operational data is taken from the two processing centres without further insight into the actual processing involved in the generation of this data. This represents the typical approach of any user interested in radio occultation data for e.g. climate

monitoring and who is external to the radio occultation community.

Several processing steps to get from the raw measurement to refractivity profiles can introduce deviations. E.g. the use of a climatology or ECMWF profiles to initialize the refractivity profile at high altitude. Within the assimilation at the Met Office, biases have been found in the surface pressure that were generated by slightly inconsistent conversions from geopotential altitudes to pressure. These biases also depend on the assimilation variable, whether it is bending angle or refractivity.

In order to perform an analysis of the two processing centres, matches of CHAMP data have to be identified. The following criteria are used to assure that a unique match is found:

1. search for CDAAC matches within $\pm$ 1 minute around the GFZ time and day
2. disregard data which do not use the same PRN satellite number
3. disregard data where the tangent points are further than 30 km apart

Additionally, the data quality flag in the CDAAC and GFZ data is used to disregard data. Based on the CDAAC flag, about 10 % of the data is rejected, although a GFZ profile was available. This also reflects the total number of bad flagging in the CDAAC data. In total there are 204,085 GFZ occultations used and 228,307 CDAAC ones; although CDAAC provides about 10 % more occultations, the bad settings removed only occultations that have a corresponding GFZ match.

We use the 200 m vertical resolution mean sea level altitudes from GFZ and spline interpolate the CDAAC data to this resolution, although we also discuss the impact of down-sampling below. Using only the time and PRN match, it is possible to relate about 165,000 occultations from GFZ with CDAAC ones. Some days are missing from the CDAAC data which are provided by GFZ, but on average there are about 20 to 30 occultations on most days which were not matched. The actual reason for this missing match was not further investigated in this report, but as [1] noted, it is interesting to also analyze the data with no match. The data without a match shows no general pattern with respect to location, time etc. Note that GFZ data was used to find a match in CDAAC and not the other way round. The lower number for GFZ mentioned above indicates more rigorous quality checks. The control for version 5 of GFZ (updates are expected soon) while CDAAC is just in the process of updating all available occultations, thus we use data as available in December 2005.

A comparison with ECMWF refractivities is shown in Figure 22. Both processing centres show similar results, although CDAAC has a lower bias at higher altitudes. Note however the restrictions discussed in Section 4 and that this is only a comparison to the ECMWF model, thus does not present a full validation with other models, radiosondes, or other satellite observations.

A comparison of global bending angles and refractivities processed at the two centres is shown in Figure 23. Generally a good bias agreement is found between the different processing centres, although small biases are visible, particularly for refractivity at high altitudes. Also, large standard deviations are found near the surface, presumably caused by different FSI processing setups. At higher altitudes, the initialization impact can be seen in the refractivity comparison. A further separation shows that land events show better agreement in bending angle and refractivity at the lowest altitudes (not shown).

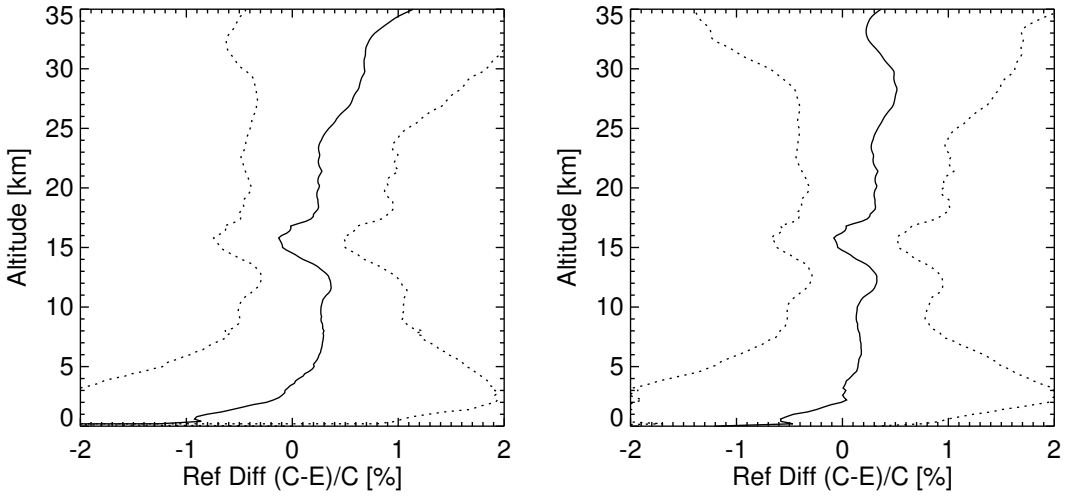

Figure 22: Comparison of CHAMP refractivities to ECMWF validation profiles, processed at GFZ (left) and CDAAC (right). GFZ and CDAAC operational data (5,000 profiles).

A latitudinal separation of the bending and refractivity profiles is presented in Figure 24, it shows that the major deviations are found at tropical latitudes at low altitudes.

One of the matching criteria was the distance between the two processing centres' tangent points. We use the mean tangent point in the 10 km to 35 km range. The actual distance of the CDAAC mean tangent point with respect to the GFZ one is shown in Figure 25. Points are plotted in a compass plane, thus one can see that most of the tangent points scatter in North-South direction which is also the direction of the main horizontal displacement (Figure 5). The mean offset is very low, although individual profiles position can vary by about 20 km, thus clearly relevant for a mesoscale model. There is also a latitude dependent offset. GFZ and CDAAC are in contact concerning these found differences, agreement with the new processing versions should improve these findings.

The mean tangent point distance does not provide information on the actual tangent point position at different altitudes. Figure 26 shows the distance separated into North–South and East–West parts as functions of altitude. Although a filter was used for the matches of 30 km in the mean distance, distances at certain altitudes can vary by a hundred kilometres, in particular at low altitudes and latitudes. The larger distance is again found in the North-South direction.

Based on the 5,000 matching profiles above, a temperature comparison is shown in Figure 27. Large biases are found especially at the upper range of the comparison, thus limiting the use for climate monitoring. The GFZ operational data used here is version 5, the next version is expected to improve temperatures. Further processing information for the two centres can be found in [8, 27].

It was mentioned above that a spline fit was used to interpolate the CDAAC profiles onto the GFZ altitude resolution. A different approach by averaging the CDAAC values over the vertical interval covered in GFZ yielded very similar results. The two interpolation methods lead to essentially no bias for all comparisons. The standard deviation between the two methods is 1 % for bending angles at low altitudes and can be up to 2 % for tropical observations.

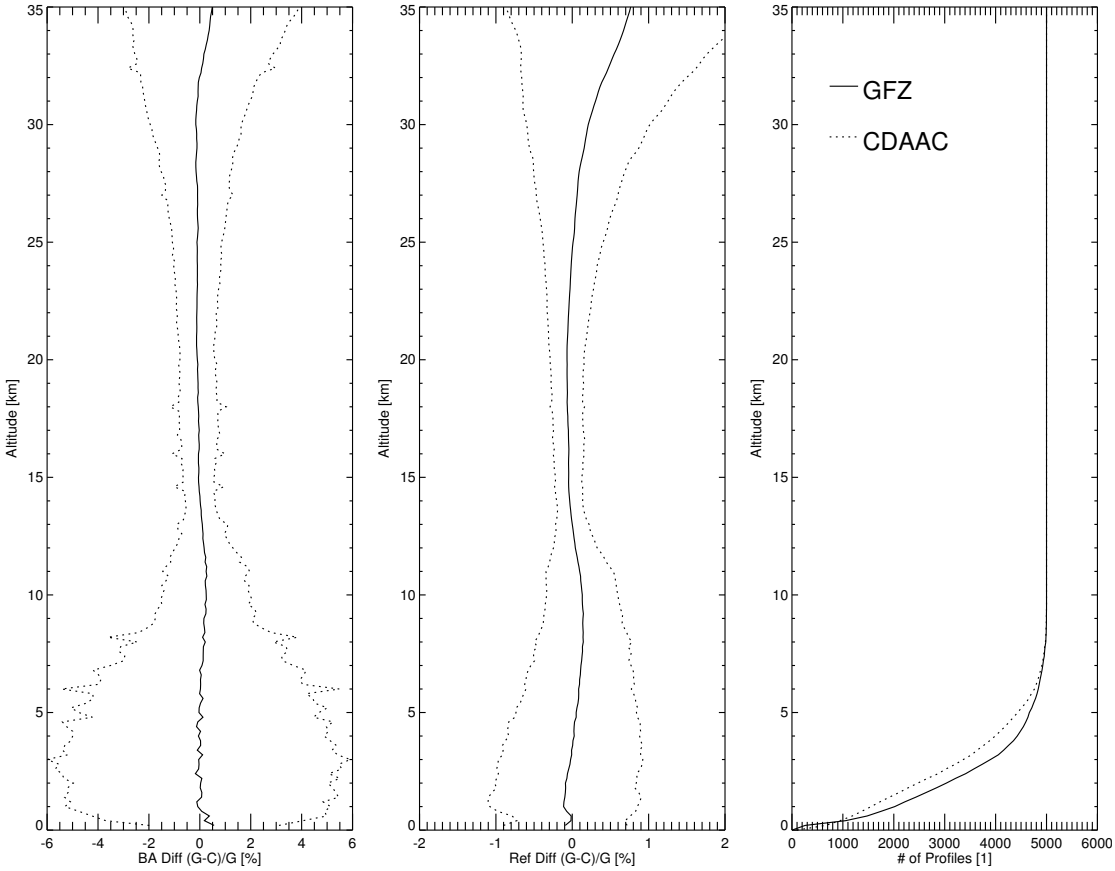

Figure 23: Comparison of bending angles (left) and refractivity (middle) profiles of GFZ and CDAAC, solid line bias, dotted line standard deviation. The right plot shows the number of profiles available at each altitude (Note: the actual number entering the statistics is always the lower of the two curves at any altitude level). GFZ and CDAAC operational data (5,000 profiles).

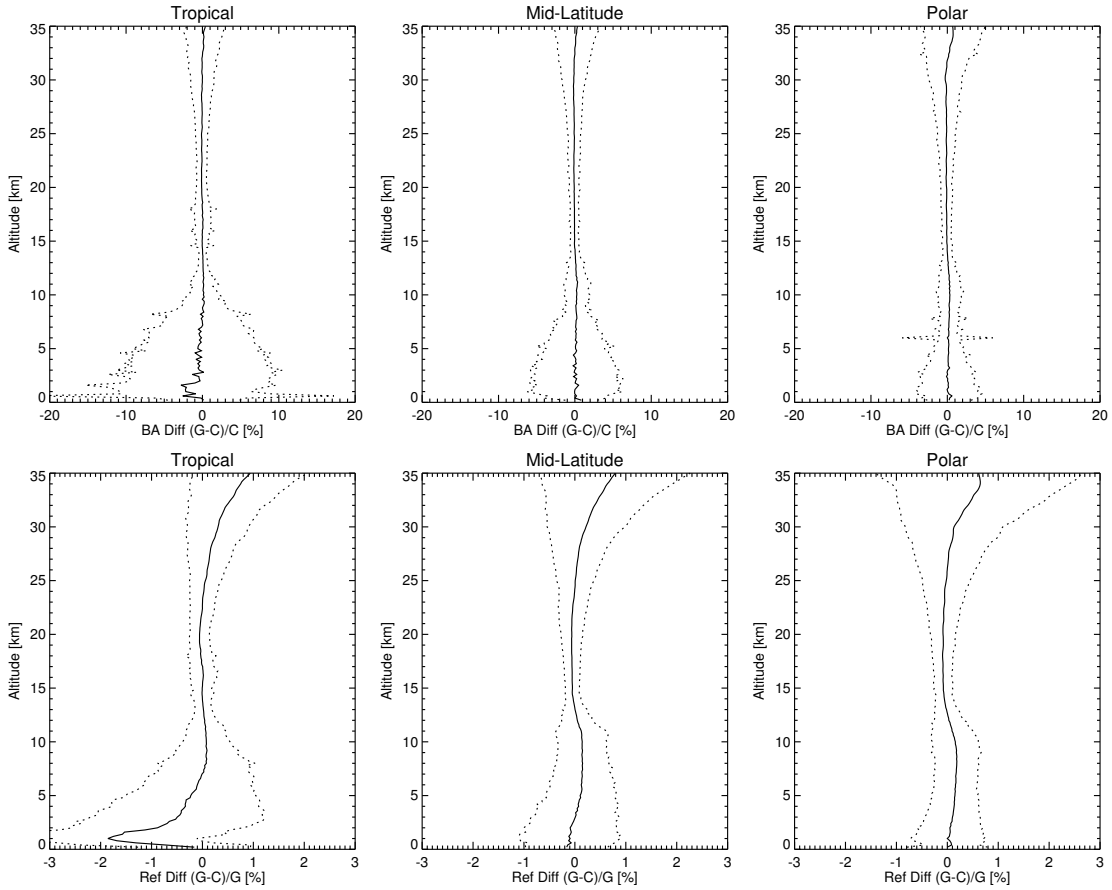

Figure 24: Comparison of bending angles (top) and refractivity (bottom) profiles of GFZ and CDAAC for different latitude bands. GFZ and CDAAC operational data (5,000 profiles).

Refractivities show standard deviations of around 0.1 % for all altitudes. Positions agree to less than a kilometre, temperatures to within 0.1 K to 0.2 K.

12 Conclusion

Radio occultation data will soon become operationally available with the GRAS and COSMIC instruments. The operational assimilation of this new data type into Numerical Weather Prediction models requires the identification and rejection of problematic data before the assimilation process. A possible approach using a 1-dimensional variational assimilation system prior to the actual assimilation into the full 3D or 4D model is discussed in [10]. Here, several other possible approaches to monitor data quality are shown. Results are not meant as a replacement of the approach suggested in [10], but are considered complimentary to it.

A general analysis of radio occultation data available from the CHAMP instrument is performed first. Data analyzed here is available from mid-2001 to June 2005, in total more than 200,000 profiles. Several different data streams have been used in this analysis where the main one is coming from GFZ (Potsdam, Germany). CHAMP data shows no homogeneous coverage with respect to area, time, or season, which might have implications for climate change and benchmarking studies, in particular when only a few occultations enter

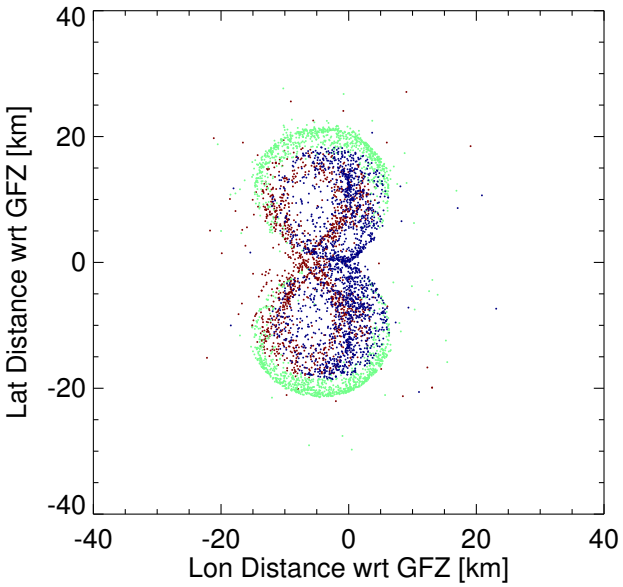

Figure 25: Tangent point distance found between the GFZ and the CDAAC mean tangent point. Red: Tropical; Green: Mid-Latitude; Blue: Polar. GFZ and CDAAC operational data (5,000 profiles).

the analysis as for example for regional studies. Although the availability of several radio occultation instruments in the near future will improve coverage. Radio occultation measurements also do not provide a vertical scan through the atmosphere; horizontal displacements can be more than 200 km in the lowest 35 km of the scan. The major movement is happening in the North–South direction caused by the general North–South movement of the CHAMP satellite.

Validation profiles co-located to CHAMP observations have been extracted from ERA 40 or ERA 40-like fields. Within this report, vertical profiles at a location weighted towards the lowest 20 km of the scan are used for validation, extracted at the nearest analysis time. An analysis of the effect of disregarding horizontal displacements and the use of the available analysis times is performed within this work. It has potential implication on the background data used in assimilation process. In particular, background data can be optimized for certain retrieval parametres such as upper stratospheric temperatures. Although the focus in NWP is more likely on the lower troposphere where horizontal variability is higher.

The amplitude of the FSI processing has been analyzed for its general behavior with respect to location and altitude. The FSI amplitude gives information on the signal strength and is affected by dominant atmospheric features such as the ITCZ. Hence these features can also be found in the vertical coverage of the CHAMP instrument where fewer occultations are penetrating into the ITCZ. The FSI amplitude shows a significant reduction in the lowest 10 km; for tropical occultations a reduction of more than 50 % is found. It also shows strong variability in the lowest few kilometres, especially for tropical occultations.

The operational threshold where processing at lower altitudes terminates is determined by the FSI amplitude set at GFZ Potsdam. The currently used threshold lies at a normalized amplitude value of 0.5. The impact of a higher or lower threshold has been assessed by running

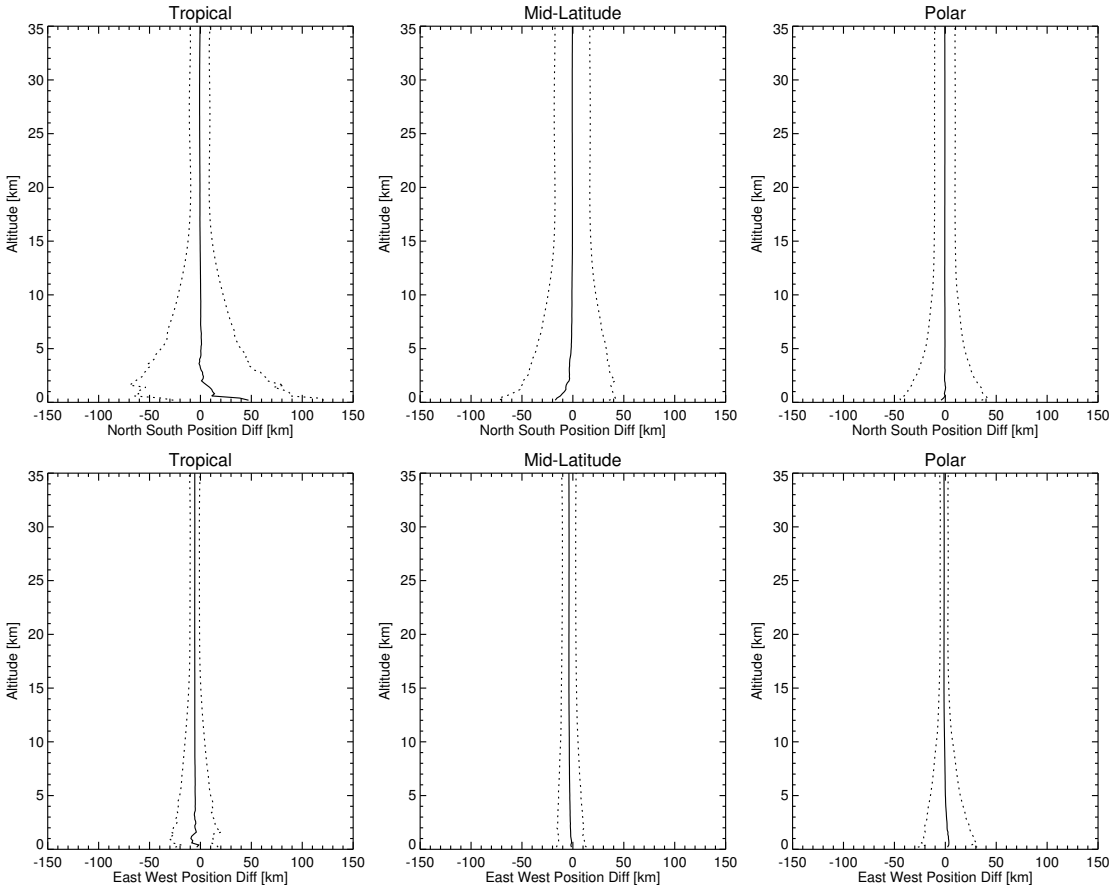

Figure 26: Tangent point distance found between the GFZ and the CDAAC for different latitude bands. Top: North-South distance; Bottom: East-West distance. GFZ and CDAAC operational data (5,000 profiles).

GFZ phase delay files through the operational processor. Using a higher threshold, and thus filtering out more occultations, leads to significantly lower refractivity biases with respect to ECMWF profiles, especially at tropical latitudes. Although the number of processed occultation at lower altitudes is reduced; tropical occultations were processed only down to about 2 km.

Altitudes where fly-wheeling (and thus short interruptions in tracking) occur have been analyzed by in-house processing of GFZ phase delay files. Very brief fly-wheeling starts even at 10 km and shows a maximum at around 7 km. In total, about 40 % of tropical occultations show brief fly-wheeling at this altitude. Longer intervals of fly-wheeling are usually associated with the surface topography or dominant atmospheric features like the ITCZ.

The ground station used in the double differencing has been used to sort and analyze occultations. A comparison with ECMWF validation profiles shows most ground stations to be in agreement, although some clearly show different statistics which might be caused by the actual occultations that are observed from this ground station. A further analysis might show whether ground stations really do influence the obtained profiles.

A similar analysis as with respect to the ground station was also performed with respect to the GPS occulting satellite. The actual plane of the GPS satellite seems to influence the

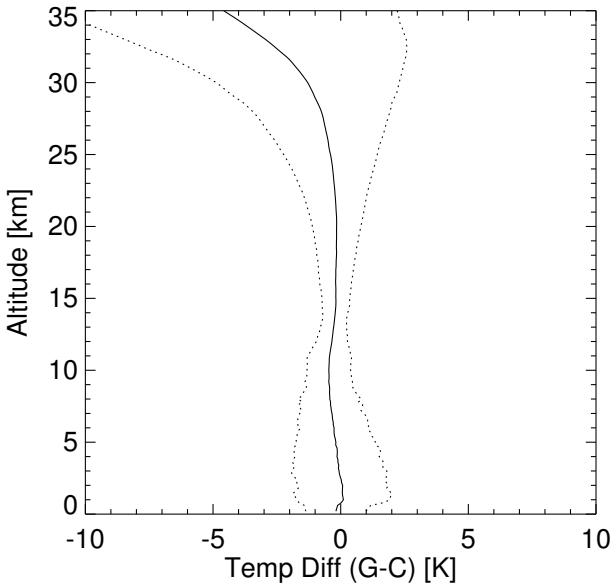

Figure 27: Temperature differences found between the GFZ and the CDAAC processing. Solid line bias, dotted line standard deviation. GFZ and CDAAC operational data (5,000 profiles).

coverage, although all involved GPS satellites show global coverage. The analysis showed some GPS satellites having fairly different statistics. Whether this is caused by the actual GPS satellite or is just caused by the slightly different coverage is unclear.

The capability of radio occultation for climate monitoring and benchmarking has already been stressed. A dataset generated for climate monitoring might consist of different radio occultation instruments which are also processed at different centres. Two centres (GFZ Potsdam and CDAAC Boulder) which process CHAMP occultations have been compared in this work to assess implications. Global results show very good agreement in refractivity and bending angle, although the different initializations used at the two centres at high altitudes to obtain the refractivity profiles lead to biases at the processing top altitude. A latitudinal separation of the results shows that larger deviations are found at tropical latitudes at low altitudes. This is presumably caused by the settings used in the FSI processing. Also, the actual tangent point as given by the two centres can vary by up to 100 km in particular at lower altitudes.

The main points that require further investigation are:

- Improvement of bending angle standard deviation agreement, mainly in the lower troposphere. This is likely caused by different FSI setups.
- Improvement of refractivity standard deviation and bias agreement. There are relatively large standard deviations found both at the lower and upper end of the scan. The lower one is likely to be FSI related, the upper one seems to stem from different initialisations, which also leads to a bias.
- Improvement in tangent point positions, in particular in the North-South direction and

at lower altitudes.

- Improvement in the total number of profiles processed. The two processing centres could maximise the number of processed occultations.

The found disagreement in temperatures is likely to disappear once the bending angle and refractivity disagreement has been resolved. Work is underway at the two processing centres to improve agreement; the currently found agreement between GFZ and CDAAC data limits the use for climate monitoring. A further analysis and comparison of processing centres is recommended. Benefits of such a thorough comparison would be:

1. Evaluate the potential of radio occultation data for climate monitoring;
2. Identify optimized data processing in the lower, moist troposphere;
3. Identify optimized processing in the upper stratosphere;
4. Provide evaluation for other processing centres;
5. Assess quality control settings of the different centres and optimize the number of processed profiles.

There is a continuation of the ROSE campaign and the GRAS-SAF is also addressing this with a visiting scientist (Armin Löscher) at DMI during 2006.

Hence a combination of radio occultation instruments to obtain a long term dataset either requires that processing centres are agreeing on one dataset of a particular instrument that can be compared with other centres (as currently done in the ROSE campaign) to assure that a combination of different centres provides consistent data. Another option is to rely on processing performed at a single centre, or one could use data that has been processed with similar settings at different centres to avoid the introduction of different biases by each processing centre. For the last option, the Radio Occultation Processing Package (ROPP) — developed within the GRAS-SAF — could serve as such common software once it has been extended to cover also the pre-processing [18].

13 Acknowledgments

Great help by the two processing centres is acknowledged in providing easy access to their data. Helpful comments and remarks by Georg Beyerle, Jens Wickert (GFZ, Potsdam), Doug Hunt, Chris Rocken, Sergey Sokolovskiy (CDAAC, Boulder), Carlo Buontempo (Met Office, Exeter) are acknowledged. Thanks to Georg Beyerle, Torsten Schmidt, and Jens Wickert (GFZ, Potsdam) for providing/processing phase delay data. Thanks to Georg Beyerle (GFZ, Potsdam) for support with his MATLAB FSI processor. Christian Marquardt (Met Office, Exeter) processed phase delay data provided by GFZ for a fly-wheeling analysis. The report was kindly reviewed by Dave Offiler and John Eyre (Met Office, Exeter)

References

[1] C.O. Ao, W.B. Schreiner, and J. Wickert. First report on the CHAMP radio occultation intercomparison study. JPL publication 03-016, JPL, 2003.

[2] G. Beyerle, T. Schmidt, G. Michalak, S. Heise, J. Wickert, and C. Reigber. GPS radio occultation with GRACE: Atmospheric profiling utilizing the zero difference technique. *Geophys. Res. Lett.*, 32, 2005.

[3] G. Beyerle, T. Schmidt, J. Wickert, S. Heise, M. Rothacher, G. König-Langlo, and K.B. Lauritsen. Observations and simulations of receiver-induced refractivity biases in GPS radio occultation. *J. Geophys. Res.*, 2005. submitted.

[4] ESA/EUMETSAT. The GRAS instrument on METOP. *ESA/EUMETSAT Rep. (ESA No. VR/3021/PI, EUM No. EPS/MIS/IN/9),* 38 p., ESA/ESTEC, Noordwijk, Netherlands, 1998.

[5] G.A. Hajj, C.O. Ao, B.A. Iijima, D. Kuang, E.R. Kursinski, A.J. Mannucci, T.K. Meehan, L.J. Romans, M. de la Torre Juarez, and T.P. Yunck. CHAMP and SAC-C atmospheric occultation results and intercomparisons. *J. Geophys. Res.*, 109, 2004.

[6] S.B. Healy and J.R. Eyre. Retrieving temperature, water vapour and surface pressure information from refractive-index profiles derived by radio occultation: A simulation study. *Q. J. R. Meteorol. Soc.*, 126:1,661–1,683, 2000.

[7] A.S. Jensen, M.S. Lohmann, H.H. Benzon, and A.S. Nielsen. Full spectrum inversion of radio occultation signals. *Radio Sci.*, 38(3):6–1 – 6–15, 2003.

[8] Y.-H. Kuo, T.K. Wee, S. Sokolovskiy, C. Rocken, W. Schreiner, D. Hunt, and R.A. Anthes. Inversion and error estimation of GPS radio occultation data. *J. Met. Soc. Japan*, 82(1B):507–531, 2004.

[9] E.R. Kursinski, G.A. Hajj, J.T. Schofield, R.P. Linfield, and K.R. Hardy. Observing Earth's atmosphere with radio occultation measurements using GPS. *J. Geophys. Res.*, 102(D25):23429–23465, 1997.

[10] C. Marquardt and S.B. Healy. WP 2.3: a strategy for the validation of GRAS level 1b data. Technical report, Met Office, March 2004. Document-No: METO/GRASVAL/03.

[11] C. Marquardt, K. Schöllhammer, G. Beyerle, T. Schmidt, J. Wickert, and Ch. Reigber. Validation and data quality of CHAMP radio occultation data. In Ch. Reigber, H. Lühr, and P. Schwintzer, editors, *First CHAMP mission results for gravity, magnetic and atmospheric studies*, pages 384–396. Springer Verlag Berlin, 2003.

[12] O. Montenbruck and R. Kroes. In-flight performance analysis of the CHAMP BlackJack GPS receiver. In *GPS Solutions*, volume 7, pages 74–86. Springer Verlag GmbH, 2003.

[13] U.S. Navy. Current GPS constellation. http://tycho.usno.navy.mil/gpscurr.html.

[14] P.I. Palmer, J.J. Barnett, J.R. Eyre, and S.B. Healy. A non-linear optimal estimation inverse method for radio occultation measurements of temperature, humidity, and surface pressure. *J. Geophys. Res.*, 105(D13):17,513–17,526, 2000.

[15] P. Poli, J. Joiner, and E.R. Kursinski. 1DVAR analysis of temperature and humidity using GPS radio occultation refractivity data. *J. Geophys. Res.*, 107(D20), 2002.

[16] C. Rocken, R. Anthes, M. Exner, D. Hunt, S. Sokolovskiy, R. Ware, M. Gorbunov, W. Schreiner, D. Feng, B. Herman, Y.-H. Kuo, and X.C. Zou. Analysis and validation of GPS/MET data in the neutral atmosphere. *J. Geophys. Res.*, 102(D25):29849–29866, 1997.

[17] C. Rocken, Y.-H. Kuo, W. Schreiner, D. Hunt, S. Sokolovskiy, and Chris McCormick. COSMIC system description. *Terrestrial, Atmospheric and Oceanic Science*, 11(1):21–52, 2000.

[18] GRAS Meteorology SAF. The Radio Occultation Processing Package (ROPP) An Overview. Technical report, Met Office, 2005. Document-No: SAF/GRAS/METO/UG/ROPP/001.

[19] A.J. Simmons and J.K. Gibson. The ERA-40 Project Plan. ERA-40 Project Report Series No. 1, ECMWF, 2000.

[20] A. von Engeln, G. Nedoluha, G. Kirchengast, and S. A. Buehler. One-dimensional variational (1-D Var) retrieval of temperature, water vapor, and a reference pressure from radio occultation measurements: A sensitivity analysis. *J. Geophys. Res.*, 108(D11):ACL 7–1 to ACL 7–13, 2003.

[21] A. von Engeln, J. Teixeira, and G. Beyerle. The impact of thin water vapor layers on CHAMP radio occultation measurements. *Radio Science*, 2005. submitted.

[22] A. von Engeln, J. Teixeira, J. Wickert, and S. A. Buehler. Using champ radio occultation data to determine the top altitude of the planetary boundary layer. *Geophys. Res. Lett.*, 32(6), 2005.

[23] J. Wickert, C.O. Ao, and W.B. Schreiner. GPS radio occultation with CHAMP: Comparison and evaluation of data analysis from GFZ, JPL and UCAR. Technical report, GeoForschungsZentrum Potsdam, 2005. Scientific Technical Report (STR), in preparation.

[24] J. Wickert, G. Beyerle, R. König, S. Heise, L. Grunwaldt, G. Michalak, Ch. Reigber, and T. Schmidt. GPS radio occultation with CHAMP and GRACE: A first look at a new and promising satellite configuration for global atmospheric sounding. *Ann. Geophysicae*, 23:653–658, 2005.

[25] J. Wickert, R. Galas, T. Schmidt, G. Beyerle, C. Reigber, C. Förste, and M. Ramatschi. Atmospheric sounding with CHAMP: GPS ground station data for occultation processing. *Phys. Chem. Earth*, 29(2-3):267–275, 2004.

[26] J. Wickert, C. Reigber, G. Beyerle, R. König, C. Marquardt, T. Schmidt, L. Grunwaldt, R. Galas, T.K. Meehan, W.G. Melbourne, and K. Hocke. Atmosphere sounding by GPS radio occultation: First results from CHAMP. *Geophys. Res. Lett.*, 28(17):3263–3266, 2001.

[27] J. Wickert, T. Schmidt, G. Beyerle, R. König, Ch. Reigber, and N. Jakowski. The radio occultation experiment aboard CHAMP: Operational data analysis and validation of vertical atmospheric profiles. *J. Meteorol. Soc. Jpn.*, 82(1B):381–395, 2004.

[28] T. Yunck, C.H. Liu, and R. Ware. A history of GPS sounding. *Terrestial Atmospheric and Oceanic Sciences*, 11(1):1–20, 2000.